DESCRIPTION: State the application's broad, long-term objectives and specific aims, making reference to the health relatedness of the project. Describe concisely the research design and methods for achieving these goals. Avoid summaries of past accomplishments and the use of the first person. This abstract is meant to serve as a succinct and accurate description of the proposed work when separated from the application. If the application is funded, this description, as is, will become public information. Therefore, do not include proprietary/confidential information. **DO NOT EXCEED THE SPACE PROVIDED.**

Our overall hypothesis is that ethanol–induced inhibition of cell adhesion, one possible cause of damage in the developing neural system, is mediated by alcohol binding sites on the L1 cell adhesion molecule. Different alcohols show remarkable structural specificity for alcohol inhibition of cell adhesion (agonist action). Other alcohols (e.g., 1-octanol) noncompetitively antagonize the effects of ethanol on L1-mediated cell adhesion and on the development of mouse whole embryo cultures. We hypothesize that these sites are on L1 because the brains of children with L1 mutations resemble those of children with fetal alcohol spectrum disorder (FASD). The novel aspect of this proposal is the use of recently developed photoaffinity alcohol analogs, 3-azibutanol (an agonist) and 3-azioctanol (an antagonist) to photolabel the agonist and antagonist binding sites respectively. Specific Aim 1 tests the hypothesis that there are alcohol agonist sites on the L1 adhesion molecule by photolabeling them with 3-azibutanol, which acts similarly to ethanol on cell adhesion. Purified L1 photolabeled with [3H]3-azibutanol will be digested and fragments photoincorporating alcohol separated by HPLC. The stoichiometry of photoincorporation will be measured by mass spectrometry. Further, digestion of target fragments will produce fragments suitable for sequencing by mass spectrometry. To assess pharmacological relevance, the apparent dissociation constant and pharmacology of each photoincorporation site will be determined and compared to those obtained from parallel cell adhesion experiments. Specific Aim 2 similarly tests the hypothesis that there are separate alcohol antagonist sites on L1 using the photoaffinity label, 3-azioctanol, which inhibits ethanol–induced inhibition of cell adhesion at micromolar concentrations. We expect to define at least one amino acid in the binding pocket of each pharmacologically well–characterized site on L1. Identification of the agonist and of the antagonist site will, respectively, aid in understanding the molecular basis for FASD and accelerate the development of drugs that block the toxic effects of ethanol on the developing nervous system.

PERFORMANCE SITE(S) *(organization, city, state)*
Massachusetts General Hospital, Boston, MA
VA Boston Healthcare system, West Roxbury, MA campus

KEY PERSONNEL. See instructions. *Use continuation pages as needed* to provide the required information in the format shown below. Start with Principal Investigator. List all other key personnel in alphabetical order, last name first.

Name	Organization	Role on Project
Miller, Keith W	Massachusetts General Hospital	PI
Arevalo, Enrique	Massachusetts General Hospital	Protein Chemist
Husain, S. Shaukat	Massachusetts General Hospital	Synthetic Chemist
Wilkemeyer, Michael F	Harvard Medical School/VA	PI, subcontract
Charness, Michael E	Harvard Medical School/VA	Co-investigator

Disclosure Permission Statement. Applicable to SBIR/STTR Only. See instructions. ☐ **Yes** ☐ **No**

A. SPECIFIC AIMS

The **overall hypothesis** is that ethanol–induced damage in the developing neural system, which results in part from inhibition of cell adhesion, is mediated by alcohol binding sites on the L1 cell adhesion molecule. This agonist action is shared by short chain alcohols, such as 1-butanol, and is noncompetitively antagonized by longer chain alcohols, such as 1-octanol. **The novel aspect of this proposal** is the use of recently developed photoaffinity alcohol analogs, 3-azibutanol (an agonist) and 3-azioctanol (an antagonist), that allow a direct search for agonist and antagonist binding sites, respectively. These photoreactive alcohols have already been employed to identify regions of certain other target proteins that mediate the actions of alcohols. The **long-term goals** of this research are a better understanding of the molecular basis for ethanol interaction with neural adhesion proteins and the rational design of safe drugs to prevent the neurotoxic effects of ethanol.

Specific Aim 1. We will test the hypothesis that there are alcohol agonist sites on the L1 adhesion molecule using a photoactive derivative of 1-butanol.

Affinity purified human L1 will be photolabeled with [^{3}H]3-azibutanol, subjected to digestion, and the fragments characterized by HPLC. To assess the pharmacological relevance of photoincorporation sites, titrations of photoincorporation and interaction with competitive and noncompetitive (allosteric) inhibitors will be compared to similar data for inhibition of cell adhesion. We have shown that 3-azibutanol inhibits L1-mediated cell adhesion (Preliminary Results).

At pharmacologically relevant sites, the amino acids where photoincorporation occurs will be determined by chromatography and mass spectrometry (LC/MS), which will reveal how many sites there are in each such fragment (stoichiometry) and by LC/MS/MS, which will provide the photoincorporation location at the primary structure level.

Specific Aim 2. We will test the hypothesis that there are alcohol antagonist sites on the L1 adhesion molecule using [^{3}H]3- and 7-azioctanol, newly developed photoreactive diazirine derivatives of octanol. We have shown that 3-azioctanol antagonizes the actions of ethanol.

Amino acids where antagonists photoincorporate, and the pharmacology of each site will be determined. The approach to be adopted parallels that for Specific Aim 1, except that antagonism of ethanol's action on L1-mediated cell adhesion will be used to assess pharmacological relevance, that is to determine which sites function as noncompetitive antagonist sites.

The extent of antagonist sites will be delineated by using 7-azioctanol, whose diazirine moiety is 5Å further away from the alcohol hydroxyl than that of 3-azioctanol, as a "molecular ruler".

B. BACKGROUND AND SIGNIFICANCE

Alcohol abuse and alcoholism cause more than 100,000 deaths [1] and cost the nation approximately $184 billion annually [2]. The effects of alcohol on the nervous system account for much of this public health burden. The recent identification of compounds that block or reduce ethanol-induced teratogenesis *in vivo* [3-5] suggests that it is feasible to develop clinically useful compounds that reduce ethanol neurotoxicity.

Molecular Targets of Ethanol

Ethanol damages both the developing and mature nervous systems [6]. Recent evidence suggests that alcohols alter nervous system function by interacting directly with selective neural proteins, including ion channels, kinases, and transporters [7, 8]. Experiments with the homologous series of 1-alcohols reveal different cutoffs for alcohol effects on diverse native and purified proteins [9-11]. For alcohols below the cutoff, potency increases as a function of increasing hydrophobicity; alcohols above the cutoff are less potent or inactive. The inactivity of 1-alcohols of greater hydrophobicity than those below the cutoff has been taken as evidence that the active 1-alcohols interact with protein rather than lipid sites [12]. The size of the alcohol cutoff and the degree of ethanol responsiveness for the $GABA_A$ and glycine receptors can be manipulated by substituting small groups or single amino acids within the transmembrane region of a protein subunit [13-16], indicating a striking degree of target specificity. Diverse alcohol targets appear to comprise a hydrophobic crevice that binds methylene groups and a hydrophilic sub-site that interacts with the hydroxyl group [17]. The observation that alcohols interact specifically with selective neural proteins suggests that one might discover specific alcohol antagonists.

Fetal Alcohol Spectrum Disorder

Fetal alcohol syndrome (FAS) is the most common preventable cause of mental retardation in the Western world [18]. Severe cases are characterized by growth deficiency, neurological abnormalities, and facial malformations and occur in approximately 5% of the offspring of alcoholic women [18, 19]. Neuropathological examination and neuroimaging reveal a spectrum of neurodevelopmental abnormalities, including hydrocephalus, partial or complete agenesis of the corpus callosum, neuronal-glial heterotopias, hypoplasia of the first five cerebellar lobules, and microencephaly [20-24]. The facial and gross mid-line brain malformations result from alcohol effects during the first trimester of pregnancy, at the time of organogenesis. Ethanol exposure during the second and third trimesters of pregnancy causes less severe birth defects, but still results in neurological, cognitive, and behavioral abnormalities, referred to as alcohol related

neurodevelopmental disorder [25]. The range of birth defects, neurological abnormalities, and behavioral syndromes associated with prenatal ethanol exposure are referred to as fetal alcohol spectrum disorder (FASD).

Molecular Mechanisms of FASD

Animal studies suggest that multiple actions of alcohol account for its teratogenicity. Important among these are inhibition of NMDA receptors [26, 27], potentiation of GABA receptors [27], disruption of the release and action of trophic and growth factors [28-36], induction of apoptosis [37-45], suppression of cell division [35, 46], and disruption of multiple pathways of signal transduction [7]. The teratogenic effects of ethanol depend both on peak ethanol concentrations and on the timing of ethanol exposure during fetal development [47-50]. Oxidative stress appears to play an important role in ethanol-induced cell death [40, 51, 52]. We have shown that ethanol inhibits cell-cell interactions mediated by the L1 cell adhesion molecule, suggesting an additional mechanism of ethanol teratogenicity [53, 54]. Inhibition of L1-mediated cell adhesion would likely disrupt a variety of critical L1-dependent developmental events, but could also provoke cell death by a process known as anoikis, the induction of apoptosis following loss of cell contact [55, 56]. Oxygen stress plays a role in anoikis [57]; hence, ethanol effects on cell adhesion could trigger anoikis through a reactive oxygen-dependent pathway [3].

The L1 Cell Adhesion Molecule: *An overview*

The L1 cell adhesion molecule is critical for normal development. At the cellular level L1 is important in axon fasciculation, growth cone guidance, neuronal migration, synaptogenesis, myelination, long-term potentiation, learning, and memory [58-61]. L1 is a multifunctional protein with both adhesive and signaling properties. Activation of L1 initiates a signaling cascade involving the FGF receptor [62] and $pp60^{c\text{-}src}$ [63], leading to changes in growth cone morphology and neurite outgrowth [64, 65].

L1 Structure-Function Relations

L1 is a transmembrane glycoprotein [66]. The extracellular domain comprises six I-set immunoglobulin (Ig) domains and five fibronectin III (FN3) repeats. A short, single-pass transmembrane domain joins with a highly conserved cytoplasmic domain. The adhesive properties of mouse L1, the chick homologue Ng-CAM, and the *Drosophila* homologue neuroglian have been mapped to portions of the extracellular domain [67-70]. Homophilic binding of human L1 is mediated by the Ig2 domain of the extracellular portion of the molecule [67, 71]; deletion of the entire cytoplasmic domain in L1 or neuroglian does not reduce adhesiveness [70, 72]. Additional Ig and fibronectin type III domains may modulate homophilic binding [73, 74]. The interaction of L1 with N-CAM molecules within the same membrane enhances the homophilic binding of L1 [75].

Two isoforms of L1 are generated by alternative splicing of a 12 base pair segment in the cytoplasmic domain encoding the amino acids arginine, serine, leucine, and glutamic acid (RSLE) [76]. The RSLE positive isoform is required for targeting of L1 to the axons and growth cones of neurons [77] and for L1-mediated cell migration [78]. The RSLE sequence and the adjacent tyrosine residue (YRSLE) interact with the AP-2 adaptor protein of clathrin coated pits, allowing for rapid internalization and recycling of L1 [79]. A second alternatively spliced region of L1 derived from exon 2 may regulate interactions of L1 with neural binding partners [80].

L1 has Multiple Binding Partners

L1 is expressed on axons and growth cones and binds to L1 molecules on adjacent cells, to components of the extracellular matrix, and to cytoskeletal elements. In addition to homophilic interactions the L1 family of adhesion molecules interact with the cytoskeletal protein ankyrin [81]. Tyrosine phosphorylation of neurofascin, a member of the L1 family, inhibits its binding to ankyrin, increases its lateral mobility, and decreases cell adhesion [82, 83]. L1 and its species homologues also bind to proteins in the extracellular matrix, including integrins, laminin, F11, axonin-1 [84, 85], and neurocan [86, 87].

L1 Mutations Cause Birth Defects

Children with mutations in the gene for L1 are mentally retarded and show a variety of neurological abnormalities described by the acronym **CRASH**: agenesis of the **C**orpus callosum, **R**etardation, **A**dducted thumbs, **S**pastic paraparesis, and **H**ydrocephalus [88]. The neuropathology of the CRASH syndrome includes to varying degrees hydrocephalus, aqueductal stenosis, hypoplasia of the first five lobules of the cerebellar vermis, hypoplasia of the corticospinal tracts, and agenesis or hypoplasia of the corpus callosum. Many of the neurodevelopmental abnormalities observed in humans with mutations in L1 are reproduced by targeted disruption of the L1 gene in mice [89]. As in humans, genetic background influences the phenotype of L1 knockout mice [89, 90]. We have noted the similarity between the brain abnormalities of children with L1 mutations and those with FAS [54]. Based on this observation, we have speculated that ethanol effects on L1 may contribute to the neurodevelopmental abnormalities of FAS.

Ethanol Effects on L1

Low concentrations (IC50 5-10 mM) of ethanol inhibit cell adhesion in an L1-expressing neural cell line (NG108-15 cells), in L1-transfected fibroblasts, and in cerebellar granule cells [53, 54]. Ethanol does not inhibit the induction of L1 or N-CAM by BMPs in NG108-15 cells; however [53], Luo and colleagues [91] reported

that ethanol reduced the induction of N-CAM by TGFß-1. Ethanol consistently inhibits cell adhesion in NG108-15 cells [4, 53, 92] and in a subset of clonal L1-transfected fibroblast cell lines [54, 93]. Ethanol does not inhibit cell adhesion in other L1-expressing fibroblast cell lines [93], myeloma cells [94], and S2 insect cells [95], suggesting that host cell factors determine ethanol sensitivity. Bearer and colleagues [94] demonstrated that low concentrations of ethanol (IC50 ~5 mM) also inhibit L1-mediated neurite extension in cerebellar granule cells. Mutated forms of L1 that cause CRASH syndrome exhibit decreased adhesion or decreased neurite induction when expressed in cultured cells [73, 96]. Hence, ethanol inhibition of L1-mediated cell adhesion and neurite extension could lead to neurodevelopmental abnormalities.

Development of Ethanol Antagonists

Structure activity analysis of various straight chain, branched-chain, and cyclic alcohols revealed surprisingly strict structural requirements for alcohol inhibition of L1-mediated cell-cell adhesion [4]. The potency of methanol, ethanol, 1-propanol, and 1-butanol increased as a function of carbon chain length and membrane-buffer partition coefficient [53, 54]. In contrast, 1-pentanol and higher 1-alcohols had no effect on L1-mediated cell-cell adhesion. The activity of 1-butanol, a four-carbon 1-alcohol, was abolished by the presence of a double bond between the 3 and 4 carbons; however, the presence of methyl groups at the 2 or 3 carbons was associated with an increase in potency [4]. These findings imply that ethanol and other small alcohols inhibit L1-mediated cell adhesion by binding within a well-defined, hydrophobic pocket of a target protein, possibly L1.

The existence of a specific binding pocket for ethanol predicts the discovery of drugs that can block ethanol's effects. Strikingly, very low concentrations of both the five-carbon alcohol 1-pentanol and the eight-carbon alcohol 1-octanol abolished the effects of ethanol on L1-mediated cell-cell adhesion [4]. 1-Octanol also blocked the effects of ethanol on the morphology of dividing neural cells [4] and prevented apoptosis and dysmorphology in cultured mouse embryos [3]. 1-Octanol is a toxic compound that could not be used clinically. However, the identification of a single compound that blocks ethanol teratogenesis suggests the possibility of safer alcohol antagonists.

Neuroprotective Peptides NAP and SAL Prevent Ethanol Teratogenesis

Recently, two neuroprotective peptides, NAPVSIPQ (NAP) and SALLRSIPA (SAL), were found to prevent ethanol-induced fetal death and growth abnormalities in a mouse model of FAS [5]. These peptides are derived from larger proteins (activity-dependent neuroprotective protein and activity-dependent neurotrophic factor, respectively), and released by glia in response to vasoactive intestinal peptide (VIP) [97, 98]. NAP and SAL are extremely potent (EC50 in the femtomolar range) neuroprotective agents [99-101], but their mechanism of action is complex and poorly understood. To better understand how NAP and SAL prevent ethanol teratogenesis, we asked whether these peptides, like octanol, antagonize ethanol inhibition of L1-mediated cell adhesion. Both NAP and SAL completely antagonized the actions of 100 mM ethanol, with half-maximal inhibition at ~10^{-14} M for NAP and at ~10^{-11} M for SAL [102]. D-NAP had the same potency as L-NAP, and structure activity analyses with L-NAP also suggested significant structural specificity. These data demonstrate that two structurally unrelated compounds, a long-chain alcohol and two small peptides, share two common actions: antagonism of ethanol inhibition of L1-mediated cell adhesion and prevention of ethanol teratogenesis.

Photolabeling of Alcohol Binding Sites

Alcohols act at such low affinity that classical pharmacological radiolabeled ligand binding studies cannot be applied [103]. The existence of alcohol binding sites has thus usually been inferred indirectly either from their allosteric effects on other more favorable ligands, or by analysis of pharmacological concentration-response curves, or by site–directed mutagenesis [104-106]. An alternative approach, photolabeling, is suggested by studies that characterized sites on the nicotinic acetylcholine receptor (nAcChoR). This receptor was first mapped using photolabels that were either cholinergic ligands (agonists or antagonists) or channel inhibitors. The former allowed the agonist sites to be located on the two alpha subunits at the alpha-delta and alpha-gamma subunit interfaces, and the latter identified the second transmembrane helices of the five pseudo–identical subunits as the cation channel's lining (M2) [107, 108].

Studies of general anesthetics acting on the nAcChoR, using rapid kinetics and site directed mutagenesis, both pointed to the existence of an alcohol site, but more direct evidence was needed to prove its existence and to locate it. Therefore, Miller and colleagues developed alcohols capable of photolabeling the nAcChoR [109]. They synthesized a novel octanol derivative, 3-azioctanol (Figure 11, Preliminary Results), which contained a diazirine moiety. Diazirines are small in size, stable under normal conditions and, when irradiated with light at wavelengths that do not damage proteins (360 nm), nitrogen dissociates leaving a carbene–bearing alcohol that covalently inserts within 10 microseconds into neighboring atoms [110, 111]. They showed 3-azioctanol to be a reversible general anesthetic *in vivo* (EC50 = 160µM) and that it enhanced GABA–induced inhibitory currents 7-fold and inhibited acetylcholine–induced excitatory currents (IC_{50} = 33 µM) [112] (see manuscript in Appendix). In short, its pharmacology was exactly like octanol's.

[^{3}H]3-Azioctanol was then employed to photolabel nAcChoRs, identifying three sites, all on the alpha subunit: one of low affinity near the acetylcholine binding pocket, another in the lipid-protein interface and a third on the second transmembrane region in what is thought to be the ion channel's lumen. Photoincorporation into the latter site was saturable and occurred when the receptor was in the desensitized, but not in its resting, conformation. Proteolytic mapping and subsequent classical amino acid sequencing identified Glu-262 in the M2 channel-lining domain to be the primary allosterically regulated site of labeling. The location of Glu-262 in the channel lumen is consistent with the inhibitory action of 3-azioctanol [113] (see Appendix). Thus, the introduction of an alcohol photolabel has proved critical to solving a long–standing problem of general anesthetic action. Subsequently, Miller and colleagues developed photolabels closer in structure to ethanol (3-azibutanol (Preliminary Results).

The identification of [^{3}H]3-butanol binding sites on L1 will help define the structural determinants for alcohol effects on a neural protein that is critical for normal development. Similarly, the characterization of [^{3}H]3-azioctanol binding sites on L1 will help reveal the molecular footprint of an ethanol antagonist site. Defining the structural basis for ethanol antagonism will greatly accelerate the search for drugs that can mitigate or prevent the teratogenic effects of ethanol.

C. PRELIMINARY RESULTS

(References associated with section headings are manuscripts included in the appendix.)

Bone Morphogenetic Proteins Regulate Neural L1 and N-CAM Gene Expression

The bone morphogenetic proteins (BMPs) are members of the TGF-ß superfamily and were first characterized for their ability to induce bone formation [114, 115]. Because the BMPs are expressed in the developing and mature nervous systems [116, 117], we investigated their effects in neural cells. We discovered that BMP-7 (OP-1) strongly induced gene and protein expression for the N-CAM and the RSLE-positive isoform of the L1 cell adhesion molecules in the NG108-15 neuroblastoma x glioma hybrid cell line [92, 118, 119]. NG108-15 cells grow separately when plated as a sub-confluent single cell suspension in serum-free medium. Supplementation of the medium for two to four days with BMP-2, BMP-4, BMP-5, BMP-6, and BMP-7 leads to the appearance of two-dimensional and three-dimensional clusters and sheets of adherent cells [118-120], referred to as BMP morphogenesis. These changes were associated with an increase in cell adhesion, as determined by a short-term re-aggregation assay.

Ethanol Inhibits BMP Morphogenesis and Cell Adhesion in Cultured Neural Cells

Cell adhesion molecules play a critical role in neuronal migration, neurite targeting, and axon fasciculation. Because the brains of children with fetal alcohol syndrome show evidence of aberrant neuronal migration [21], we asked whether ethanol would disrupt BMP morphogenesis in NG108-15 cells. Ethanol (IC50, 5-10 mM) strongly inhibited BMP morphogenesis without reducing the rate of cell division or inducing cell differentiation [53, 92], suggesting that this effect was related to the common action of BMPs to induce L1 and N-CAM gene expression. Ethanol did not reduce the induction, gel mobility, or cell surface expression of N-CAM or L1 in BMP-treated cells [53]. These data suggested that ethanol inhibited BMP morphogenesis by disrupting the function of L1 and N-CAM. The effects of ethanol on BMP morphogenesis were not reproduced by teratogenic concentrations of phenylalanine, valproic acid, or phenytoin [53], indicating that inhibition of cell adhesion is not a common action of all teratogens. To explore the possibility that ethanol inhibits the cell-cell interactions of BMP-treated cells, we studied the effects of brief (30 minutes) ethanol exposure on calcium-independent cell adhesion. Ethanol caused a dose-dependent inhibition of calcium-independent cell adhesion [53]. The half-maximal concentration for this effect, 5-10 mM, was similar to that observed for ethanol inhibition of BMP morphogenesis.

Ethanol Inhibits Cell Adhesion in Fibroblasts Transfected with Human L1 [54]

While doing these early experiments, publications first appeared suggesting that a diverse group of developmental abnormalities were caused by mutations in the gene for L1. Some of these abnormalities, which are now grouped together as the CRASH syndrome, bore a striking resemblance to FAS. In particular, the brains of children with both the CRASH syndrome and FAS show hydrocephalus, agenesis or dysgenesis of the corpus callosum, and dysplasia of the first five lobules of the cerebellar vermis. We therefore asked whether ethanol inhibits cell adhesion mediated by L1, N-CAM, or both. We stably transfected mouse L cell and NIH/3T3 fibroblasts with an expression vector containing the human gene for L1 or with the empty vector [54]. L1-transfected cells showed higher levels of cell adhesion than wild-type or vector-transfected cells. Ethanol caused a dose-dependent decrease in the cell adhesion of L1-expressing cells (2A2-L1 cells), but had no effect on the lower levels of adhesion of wild-type or vector-transfected cells. Half-maximal inhibition occurred at an ethanol concentration of approximately 7 mM. Neither acetaldehyde nor acetate inhibited cell adhesion, suggesting that ethanol was acting directly, rather than through the production of metabolites. In contrast, ethanol did not inhibit cell adhesion in NIH/3T3 cells transfected with the human gene encoding the 140 kDa isoform of N-CAM [54].

Ethanol Inhibits Adhesion of Cerebellar Granule Cells to L1-transfected Fibroblasts [54]

We next asked whether ethanol inhibits L1-mediated adhesion of central nervous system neurons. Cerebellar granule cells express both L1 and N-CAM [121, 122]. We labeled post-natal day 8 rat cerebellar granule cells with the fluorescent dye, DiI and allowed them to adhere to a monolayer of fibroblasts transfected with human L1, human N-CAM-140 or the empty expression vector. The monolayer was then washed gently and the adherent cells were counted. Cerebellar granule cells adhered better to monolayers of N-CAM-140 and L1-expressing fibroblasts than to the empty vector-transfected fibroblasts. Ethanol inhibited the adhesion of cerebellar granule cells to the L1-expressing monolayer, but not to the N-CAM-140 or empty vector monolayers. Ethanol inhibition was dose-dependent and showed the same dose-response curve as that observed for ethanol inhibition of cell adhesion in L1-expressing fibroblasts and in BMP-treated NG108-15 cells. These data indicate that ethanol selectively inhibits cell-cell adhesion mediated by L1.

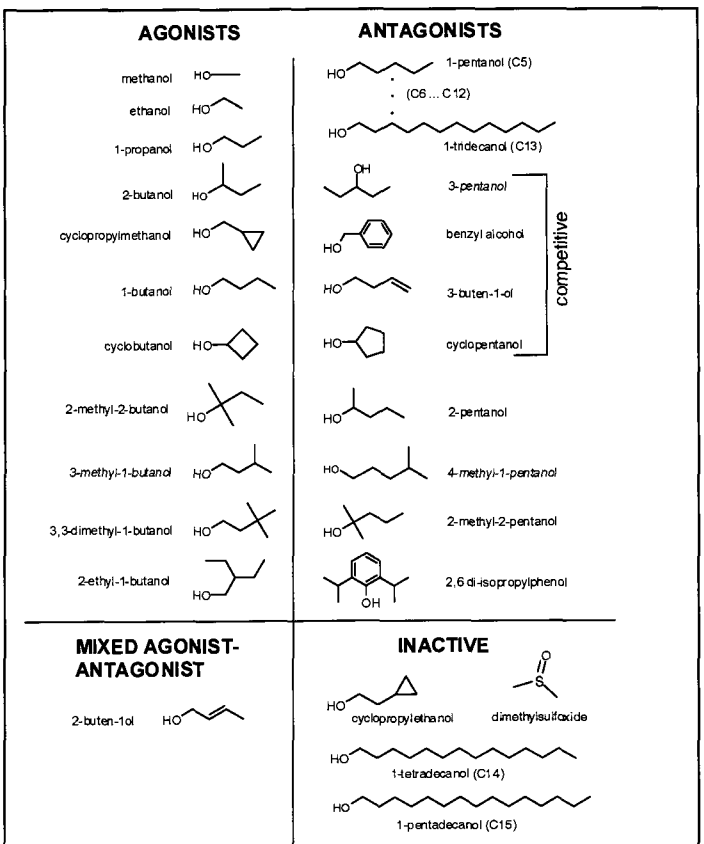

Figure 1. Structure activity relation of alcohols
Alcohols are categorized as *agonists* (inhibit L1-mediated cell adhesion), *antagonists* (block the actions of agonists), *mixed agonist-antagonists* (inhibit L1-mediated cell adhesion at lower potency than predicted with weak antagonist activity at low concentrations) or *inactive* (having neither agonist nor antagonist activity). Competitive antagonists are bracketed.

Mutations in the gene for L1 occur throughout the coding region and are likely to affect both cell adhesion as well as L1-mediated cell signaling [60]. In fact, at least two mis-sense mutations in the second Ig domain of L1 have been shown to disrupt L1-mediated adhesion [96]. Hence, our data suggest that disruption of L1-mediated cell adhesion is one possible mechanism for the overlapping neuropathologic features of L1 mutation and fetal alcohol exposure.

Quantitative Structure Activity Analysis of Alcohol Inhibition of L1-mediated Cell Adhesion[4]

To explore the mechanism by which ethanol inhibits cell adhesion, we tested a series of alcohols in ethanol-sensitive L1-transfected fibroblasts (2A2-L1 and 2B2-L1) and in BMP-7-treated NG108-15 cells [4]. Figure 1 depicts the chemical structure of alcohols that inhibited L1-mediated cell adhesion (herein referred to as **agonists**). For each alcohol studied, similar results were obtained in BMP-7-treated NG108-15 cells and in L1-expressing NIH/3T3 cells. L1-mediated cell adhesion was inhibited with increasing potency by methanol, ethanol, 1-propanol, and 1-butanol [53, 54]. In contrast, all 1-alcohols larger than 1-butanol (C4) (from 1-pentanol (C5) to 1-pentadecanol (C15)) failed to inhibit cell adhesion, even at concentrations that produce membrane disordering equivalent to 300 mM ethanol [123]. We also observed a cutoff for cyclic alcohols: cyclobutanol was an agonist; cyclopentanol and benzyl alcohol were not. The presence of an abrupt cutoff suggests that short-chain 1-alcohols interact with a hydrophobic recognition site of limited dimensions.

Alcohols as Multivalent Ligands [4]

The target site also appears to discriminate among structurally related alcohols. 1-Butanol was both the most potent 1-alcohol but also the most constrained, it's activity being readily altered by minor chemical modifications. Restriction of movement between the 3 and 4 carbons of 1-butanol (e.g., 3-buten-1-ol or cyclopropylethanol) or the placement of methyl groups adjacent to the hydroxyl group of 1-butanol (e.g. 2-pentanol and 2-methyl-2-pentanol) abolished agonist activity [4]. These findings imply that interactions near the number 1 and 4 carbons of 1-butanol are critical for agonist activity.

In contrast, the presence of methyl or ethyl groups at the 2 or 3 carbons increased agonist potency, as observed for 3-methyl-1-butanol, 2-ethyl-1-butanol, or 3,3-dimethyl-1-butanol. Dose response curves for inhibition of cell adhesion were analyzed in BMP-7 treated NG108-15 cells. Maximal inhibition of cell adhesion was comparable for all four alcohols. The potency of agonist activity, however, differed by several fold (Figure 2). It increased as a function of the number of 1-butanol moieties rather than the molecular volume or the membrane/buffer partition coefficient [4]. The EC50 values for inhibition of cell adhesion were as follows: 1-

butanol, 350 μM; 3-methyl-1-butanol, 290 μM; 2-ethyl-1-butanol, 230 μM and 3,3-dimethyl-1-butanol, 50 μM.

If alcohol agonists have strict structural requirements, then it is likely that potent alcohols, such as 1-butanol, must align with the target site in a specific orientation to inhibit cell adhesion. 3-methyl-1-butanol and 2-ethyl-1-butanol can each present a butanol moiety from two separate alignments, whereas 3-dimethyl-1-butanol has three possible alignments. These three alcohols may be more potent than 1-butanol, because they are multivalent ligands that can present a 1-butanol moiety to a target site from two or three different orientations [4]. These data will be useful in the photolabeling experiments as the more potent butanol derivatives could be used for competition studies to show specificity of azibutanol binding (Section D).

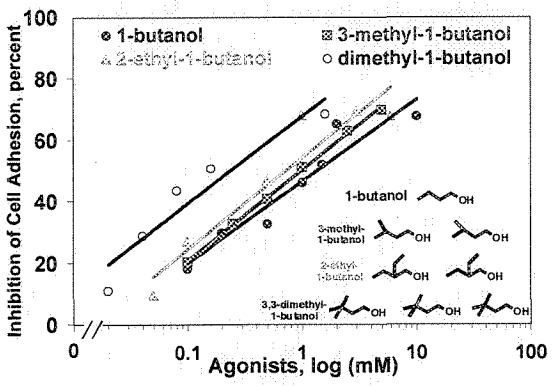

Figure 2. Relation between the number of 1-butanol moieties and the potency for alcohol inhibition of cell adhesion. Shown are the mean percentages for inhibition of cell adhesion by the indicated alcohols using BMP-7 treated NG108 cells (n=3-6). Lines are fit by log-linear regression analysis. *Insert* - The location of butanol molecules within the parent structures are outlined in red.

Hypothetical Agonist Binding Site

These structure–activity analyses suggested the existence of an agonist target site comprising a discrete hydrophobic binding sub–site adjacent to a hydrophilic sub–site. Agonist effects may occur only when a molecule binds to the hydrophobic sub–site and orients its hydroxyl group towards the hydrophilic sub–site. The agonist target can be envisioned as a 1-butanol receptor that narrowly accommodates a flexed 1-butanol molecule. Restricting movement between the 3 and 4 carbons of 1-butanol may abolish agonist activity by preventing bound 1-butanol from presenting its hydroxyl group to the hydrophilic sub–site. An extended conformation of 1-butanol (3-buten-1-ol) or longer 1-alcohols (e.g. 1-pentanol) may be inactive as agonists because they are unable to bind coordinately to closely spaced hydrophobic and hydrophilic sites. Methanol, ethanol, and 1-propanol may be less potent than 1-butanol, because they are less hydrophobic and bind with lower affinity to the hydrophobic site. However, because they are small enough to maintain the correct orientation between their hydrophobic methylene groups and hydrophilic hydroxyl groups, they are still agonists. The most straightforward explanation for these results is that the agonist binding site is on L1. The research proposed in this grant is aimed at testing this hypothesis.

Long-chain Alcohols Antagonize the Effects of Short-chain Alcohols on Cell Adhesion [4]

The structural specificity of the agonist target site was consistent with a ligand-receptor interaction, which suggested the possibility of identifying antagonists. We first evaluated non-agonist 1-alcohols longer than 1-butanol, based on the notion that they might compete with the hydrophobic portion of the agonist binding site. Both 1-pentanol and 1-octanol completely abolished the agonist effects of ethanol and 1-butanol in L1-expressing NIH/3T3 cells (2A2-L1) (Figure 3) and in BMP-treated NG108-15 cells [4]. Antagonism was dose-dependent, and 1-octanol (IC_{50}=3.6 μM) was approximately 200 times more potent than 1-pentanol (IC_{50}=715 μM). 1-Octanol antagonism was fully reversible and was only partly reduced by increasing concentrations of 1-butanol, consistent with a non-competitive mechanism of action. Antagonism was also functionally significant; because 1-octanol significantly antagonized ethanol inhibition of BMP morphogenesis in NG108-15 cells [4].

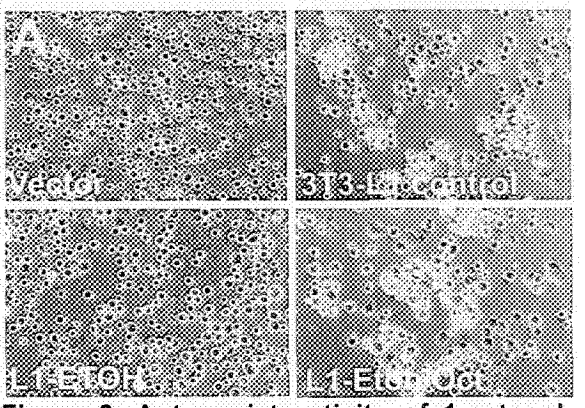

Figure 3. Antagonist activity of 1-octanol. Cell adhesion assays were performed with empty vector-transfected (Vec) or human L1 transfected (3T3-L1) NIH/3T3 cells in the absence or presence of 100 mM ethanol (L1-ETOH) or ethanol plus 50μM octanol (L1-Etoh/Oct). Ethanol reduced cell adhesion to levels found in vector cells, while octanol blocked this inhibition, returning cell adhesion to control levels.

1-Octanol Antagonizes Ethanol Toxicity in Whole Embryo Culture[3]

We next asked whether 1-octanol could prevent ethanol teratogenesis in mouse whole embryo culture. Embryos (E8, 3-5 somites) were cultured for 6 hours in the absence and presence of alcohols and transferred to control medium for an additional 20 hours. Somite pairs

were counted after a total of 26 hours in culture. Based on somite counts, treatment with 3 μM 1-octanol did not produce a delay in embryonic development, whereas 10 μM and 50 μM 1-octanol caused increasing toxicity. Embryos cultured for 6 hours with 100 mM ethanol showed markedly delayed *in vitro* development (13.2±0.6 somite pairs after 26 hours, n = 23) as compared with control embryos (19.1±0.4 somite pairs, n = 18). The toxicity of 100 mM ethanol was significantly reduced by co-incubation with 3 μM 1-octanol (16.9±0.6 somite pairs; n=23, $p < 0.001$) (Figure 4). Ethanol also increased apoptotic cell death in the lateral margins of the cranial neuroepithelium, including the region of the pre-migratory neural crest, as determined by Nile blue sulfate and Tunel staining. 1-Octanol strikingly reduced ethanol-induced apoptosis. PCR and immunohistochemistry showed evidence for the non-neuronal isoform of L1 in E8 embryos. These data demonstrate that 1-octanol reduces ethanol-induced cell death and dysmorphology in whole embryo culture and support the role of L1-mediated adhesion.

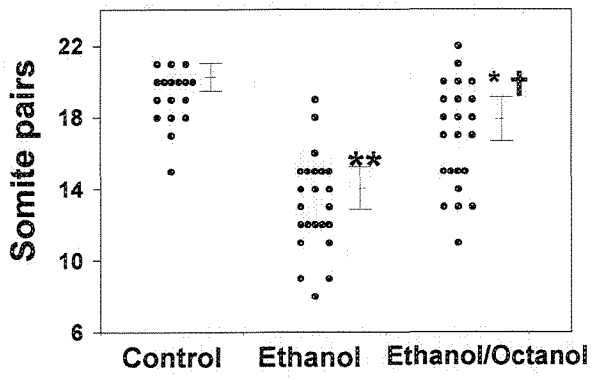

Figure 4. Effect of 1-octanol and ethanol on the morphology of cultured C57Bl/6J GD8 mouse embryos. Shown are the mean ± 95% confidence interval and number of somite pairs in individual embryos treated for 6 hours under control conditions (n=18), in the presence of 100 mM ethanol alone (n=23), or with 100 mM ethanol combined with 3 μM 1-octanol (n=23) and following an additional 20 hours of culture.
* p<0.001, ethanol plus octanol vs ethanol alone;
** p<0.001, ethanol vs control;
† p=0.024, ethanol plus octanol vs control

Multiple Ethanol Antagonists [124]
Because 1-octanol had a very low therapeutic index (toxicity just above the effective dose) [3], we searched for other ethanol antagonists. Each candidate antagonist was first tested at a single aqueous concentration that was calculated to produce an estimated molar membrane concentration equivalent to 100 mM ethanol (EC_{EQ}). Figure 1 shows the structure of the alcohols tested for antagonist activity. Most of the candidate molecules blocked more than 60% of the activity of 100 mM ethanol or 2 mM 1-butanol [124]. In contrast, DMSO, cyclopropylethanol, 1-tetradecanol, and 1-pentadecanol were neither agonists nor antagonists.

Structure-Activity Analysis of Alcohol Antagonists [124]
As with the agonist compounds, the antagonist alcohols exhibited interesting structure-function relations. For example, 3-buten-1-ol differs from 1-butanol only by the presence of a double bond between the number 3 and 4 carbon atoms. Alone, 3-buten-1-ol had no effect on L1-mediated cell-cell adhesion [4]; however, 9.6 mM 3-buten-1-ol (EC_{EQ}) blocked 64±16% of the agonist activity of 100 mM ethanol. The presence of a double bond between the 2 and 3 carbons in 1-butanol had a different effect. At a concentration of 15 mM (EC_{EQ}), 2-buten-1-ol partially inhibited L1-mediated cell adhesion, but also partially antagonized the actions of 1-butanol and ethanol [124]. At higher concentrations (150 mM), 2-buten-1-ol maximally inhibited L1-mediated cell adhesion and neither antagonized nor augmented the actions of 1-butanol or ethanol. Hence, the presence and position of a double bond determined whether the resulting molecule is a potent agonist (1-butanol), a mixed agonist-antagonist (2-buten-1-ol), or a competitive antagonist (3-buten-1-ol) (Figure 1).

We also asked if there was a cutoff for the antagonist effect of long-chain 1-alcohols. A series of 1-alcohols were dissolved in 1% DMSO to avoid problems with aqueous solubility. Antagonist potency increased progressively over 5 log orders from 1-pentanol (C5) to 1-undecanol (C11) using our human L1-expressing NIH/3T3 cells (2A2-L1) (Figure 5). The potency of 1-dodecanol (C12) was slightly less than that of C11, whereas 1-tridecanol (C13) was approximately 25 fold less potent than C12. 1-Tetradecanol (C14) showed only minimal antagonist activity and 1-pentadecanol (C15) was completely inactive. The presence of a gradual cutoff between C11 and 13 suggests that antagonist alcohols also interact with a hydrophobic pocket of limited size.

A Multivalent Antagonist [124]
Molecules that contain multiple representations of 1-butanol are more potent agonists than 1-butanol [4], consistent with the hypothesis that agonists interact with a selective recognition site. If the antagonist site is similarly selective, then molecules that contain multiple representations of an antagonist should be more potent than the antagonist itself. In this model, 4-methyl-1-pentanol can present a 1-pentanol molecule to a putative antagonist site from two different orientations (Figure 6,). Concentration-response curves were determined for 1-pentanol and 4-methyl-1-pentanol antagonism of 2 mM butanol inhibition of L1-mediated cell adhesion. 1-Hexanol was used as a control for the number of carbons in 4-methyl-1-pentanol. Antagonist potency was

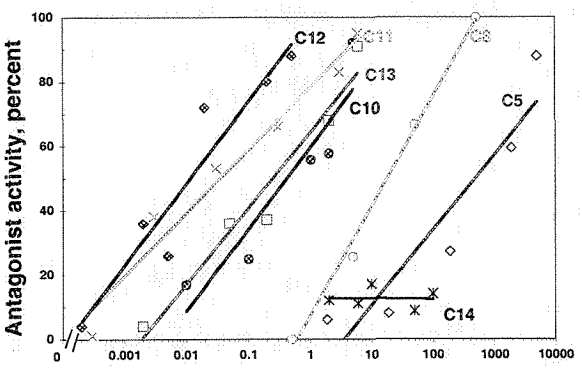

Figure 5. Antagonist effects of long-chain alcohols. Cell adhesion assays were performed in L1-expressing NIH/3T3 cells in the presence of ethanol (100 mM) and the indicated aqueous concentrations of alcohol antagonists. Shown are the means for the antagonist activity (n = 4-16). Lines are fit by log-linear regression. Shown below in parentheses are the EC_{50}s (μM) . Blue diamond: C5, 1-pentanol (540); open green circle: C8, 1-octanol (3); filled red circle: C10, 1-dodecanol (0.4); green cross: C11, 1-undecanol (0.03); filled red diamond: C12, 1-dodecanol (0.01); open blue square: C13, 1-tridecanol

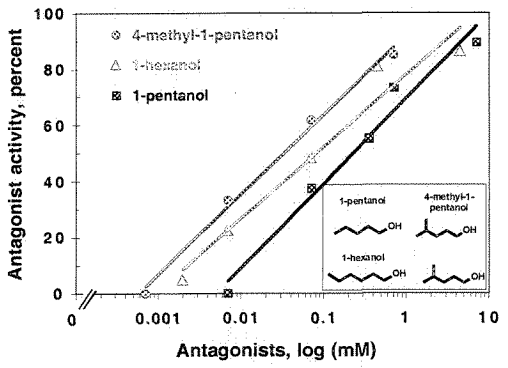

Figure 6. Antagonism of 1-butanol effects by 1-pentanol, 1-hexanol, and 4-methyl-1-pentanol (4MP). Cell adhesion assays were performed in 2A2-L1 cells in the presence of 1-butanol (2 mM) and the indicated concentrations of 1-pentanol, 1-hexanol, or 4-MP. Shown is the mean antagonist activity. Note that 4-methyl-1-pentanol, which can present a 1-pentanol moiety from two possible orientations, is approximately 4 fold more potent than 1-pentanol. *Insert* - The location of pentanol molecules within the parent structures is outlined in red.

estimated from a linear regression analysis of the antagonist concentration-response curves (Figure 6). The aqueous concentration of 4-methyl-1-pentanol that produced half maximal effect (32 μM) was approximately 7-fold greater than that of 1-pentanol (223 μM), and approximately 2.5 times that of 1-hexanol (80 μM) (Figure 6). These ratios were then adjusted, based on estimated membrane buffer partition coefficients, to take into account the difference in membrane concentration of each antagonist. With this correction, 4-methyl-1-pentanol was approximately 3.7-fold more potent than 1-pentanol, whereas 1-hexanol was only 0.7-fold as potent as 1-pentanol. This observation is consistent with the existence of a selective antagonist recognition site, that we hypothesize is on L1.

Mechanisms of Antagonism. [124]

We used our 2A2-L1 cell line to first investigate the mechanism of inhibition for two structurally dissimilar antagonists, 3-buten-1-ol and 1-octanol. Increasing concentrations of 1-butanol progressively reduced and then eliminated the antagonist effect of 3 mM 3-buten-1-ol. In contrast, increasing concentrations of 1-butanol did not eliminate the antagonist effect of 5 μM 1-octanol [124]. These experiments suggest that ethanol inhibition of L1-mediated cell adhesion can be antagonized through surmountable or non-surmountable mechanisms. We extended these experiments to a total of 10 different antagonists, each of which was tested at a concentration that blocked 50% to 80% of the actions of 2 mM 1-butanol. Increasing concentrations of 1-butanol eliminated the antagonist activity of 3-pentanol, cyclopentanol, benzyl alcohol, and 3-buten-1-ol (Figure 1). In contrast, concentrations of up to 75 mM butanol, the highest concentration tolerated by these cells, did not eliminate the antagonist activity of 2-methyl-2-pentanol, 1-octanol, 1-pentanol, 2-pentanol, 4-methyl-1-pentanol and 2,6-di-isopropylphenol (propofol)[124]. The observation that alcohol antagonists act through surmountable or non-surmountable mechanisms raises the possibility that there may be multiple sites or mechanisms of antagonist action.

NAP and SAL are Potent Antagonists of Ethanol. [102]

Coincident with our observations that 1-octanol antagonizes ethanol teratogenesis in whole embryo culture [3], Spong and colleagues [5] demonstrated that the neuroprotective peptides NAP (**NAP**VSIPQ) and SAL (**SAL**LRSIPA) prevent ethanol-induced growth retardation and fetal wastage. To explore the cellular mechanism underlying this phenomenon, we asked whether NAP and SAL could antagonize ethanol inhibition of L1-mediated cell adhesion [102]. We first used our 2A2-L1 cell line to determine the effects of the peptides on L1-mediated cell adhesion and ethanol-inhibition of that adhesion. As shown in Figure 7, both NAP and SAL were potent and complete ethanol antagonists (EC50, NAP ~10^{-14}M SAL~10^{-11}M, as determined by linear regression analyses of the dose-response curves). Addition of either peptide in the absence of ethanol had **no** effect on L1-mediated cell adhesion. A concentration-response curve revealed that NAP was also a potent antagonist for ethanol inhibition

of cell adhesion in BMP-7 treated NG108-15 cells, with nearly maximal antagonist activity at a concentration of 100 nM (mean ± SEM = 92 ± 5%; n=4). Scrambled versions of the NAP peptide (PNIQVASP and ASPNQPIV) were not effective antagonists, nor did they effect cell adhesion [102].

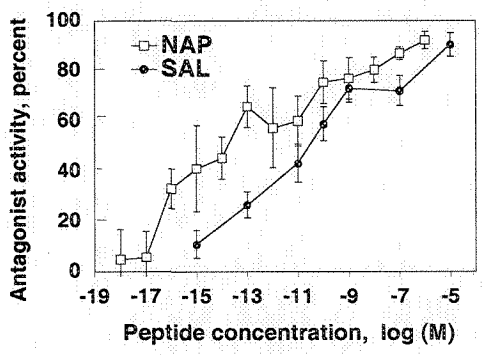

NAP = NAPVSIPQ
SAL = SALLRSIPA

Figure 7. NAP and SAL are potent antagonists. Cell adhesion assays were performed with 2A2-L1 cells in the presence of 100 mM ethanol and the indicated concentration of L-NAP or L-SAL. Shown is the mean ± SEM percent antagonist activity for the indicated peptide (n=20).

Mechanisms of NAP and SAL Activity [102]

To further explore the pharmacology of the peptides we asked whether NAP and SAL antagonism could be overcome by increasing concentrations of agonist. For these studies we again used our 2A2-L1 cell line (L1-transfected NIH/3T3 cells). Adhesion assays were performed in the presence of increasing concentrations of ethanol and a fixed concentration near the EC50 for NAP (10^{-13}M) or SAL (10^{-10} M). As shown in Figure 8, 10^{-10} M SAL greatly reduced the inhibition of L1 adhesion by 100 mM ethanol. The antagonist activity of 10^{-10} M SAL was reduced progressively when assays were conducted in the presence of increasing concentrations of ethanol and eliminated with 400 mM ethanol. In contrast, the antagonist activity of 10^{-13} M NAP was similar in the presence of 100 mM or 400 mM ethanol [102]. NAP and SAL also showed differences in the reversibility of their actions. Pre-treatment of cells with SAL (10^{-10} M) for 30 minutes, followed by extensive washing only partially reduced ethanol inhibition of L1-mediated cell adhesion. In contrast, ethanol did not inhibit L1 adhesion in cells that were pretreated with NAP (10^{-13} M) and then washed extensively [102].

Together, these data suggest that the antagonist activity of SAL is reversible and surmountable, whereas that of NAP is irreversible and non-surmountable, at least over the time course of these experiments. SAL in particular will be an important reagent for the experiments outlined in section D. We will use it as a potential allosteric modulator of L1 function and as one criteria for whether photoincorporation of azibutanol to L1 has functional significance.

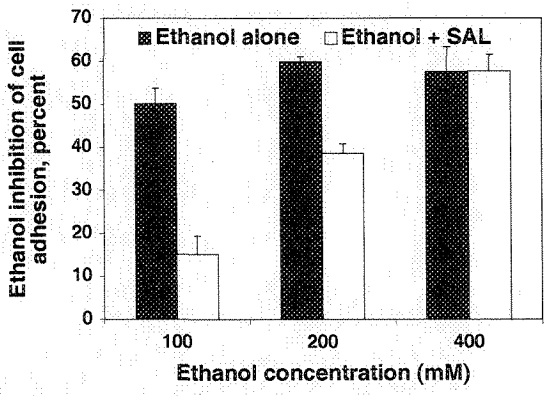

Figure 8. Effect of increasing agonist concentration on SAL antagonist activity. Cell adhesion assays were performed with NIH/3T3 cells expressing human L1 (2A2-L1) in the presence of increasing concentrations of ethanol and SAL. Shown are the mean ± SEM for the percent inhibition of cell adhesion by ethanol alone (dark bar) by ethanol plus 10^{-10} M SAL (white bar). 100 mM ethanol produces near maximum inhibition of cell adhesion. (N=3-8).

NAP Prevents Ethanol-induced Developmental Toxicity.

Like 1-octanol, NAP prevents ethanol-induced growth retardation in mouse whole embryo culture [125]. A single concentration (100 pM) of NAP was tested in mouse whole embryo culture. GD8.5 mouse embryos (3-5 somites) were cultured for 6 hours in control medium in the absence or presence of 100 mM ethanol or peptide plus ethanol and then transferred to control medium for an additional 20 hours [3]. Somite pairs were counted after a total of 26 hours in culture. As shown in Table 1 and Figure 9A, embryos cultured for 6 hours with 100 mM ethanol showed markedly delayed *in vitro* development as compared with control embryos. The co-incubation of cultured embryos with NAP, however, significantly reduced ethanol-induced growth reduction.

TABLE 1

	Control	EtOH	EtOH/NAP
MEAN # of somites	20.4	14.2	19.4
SEM	0.5	0.4	0.8
N	13	44	17

Effect of ethanol and NAP peptides on cultured C57Bl/6J GD8 mouse embryos. Shown are the mean ± SEM number of somite pairs in individual embryos treated for 6 hours under control conditions (n=13), in the presence of 100 mM ethanol alone (EtOH n=44), or with 100 mM ethanol combined with 100 pM NAP (EtOH/NAP, n=17). [125]

Table 2

NAP-derived peptides		Maximal Effect %			EC50 (fM)	EC50 (fM)	EC50 (pM)
		L1	TTX	TTX	L1	TTX	TTX
			P1	P2		P1	P2
NAPVSIPQ	(NAP)	96 ± 4	100 ± 2	97 ± 4	36	0.003	3
AAPVSIPQ	(N1A)	88 ± 4	89 ± 3	101± 3	69	0.1	100
NAAVSIPQ	(P3A)	92 ± 6	95 ± 2	89 ± 2	46,000	100	300
NAPASIPQ	(V4A)	92 ± 8	95 ± 2	96 ± 4	90,000	3	3
NAPVAIPQ	(S5A)	79 ± 8	0	0	19,000	-	-
NAPVSAPQ	(I6A)	50 ± 10	91± 1	91± 2	700,000	3	3000
NAPVSIAQ	(P7A)	76 ± 5	0	0	50,000	-	-
NAPVSIPA	(Q8A)	93 ± 7	97 ± 1	98 ± 2	4,400	0.003	3

Table 2. Comparison of structure activity relation for NAP antagonism and NAP neuroprotection. NAP potency and efficacy were estimated from dose response curves for NAP antagonism of ethanol inhibition of L1 adhesion and NAP protection of neuronal cultures from TTX toxicity. NAP potency for ethanol antagonism was calculated from linear regression analysis of the dose response curves. NAP potency for neuroprotection was estimated from the two peaks (P1 and P2) of the dose response curves. "L1" refers to NAP antagonism of ethanol inhibition of L1 adhesion. "TTX" refers to NAP protection of cortical neurons from TTX toxicity.

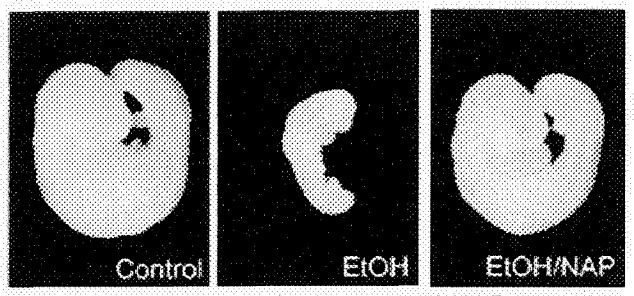

Figure 9 A. Effect of ethanol and NAP peptides on cultured C57Bl/6J GD8 mouse embryos. A. Illustrated is a representative embryo (median number of somites) from each of the five experimental groups: Control, 21 somites; Ethanol (EtOH), 14 somites; Ethanol plus NAP (EtOH/NAP), 20 somites.

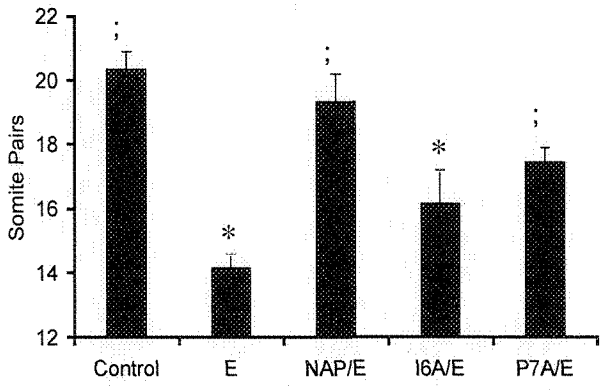

Figure 9 B. Effect of ethanol and NAP peptides on cultured C57Bl/6J GD8 mouse embryos. B. Shown are mean ± SEM number of somite pairs in individual embryos treated for 6 hours under control conditions (n=13), in the presence of 100 mM ethanol alone (E, n=44), or with 100 mM ethanol combined with 100 pM NAP (NAP/E, n=17), I6A-NAP (I6A/E, n=23), or P7A-NAP (P7A/E, n=28) and following an additional 20 hours of culture.
† $p<0.0001$, compared to ethanol alone
* $p<0.0001$, compared to control

Differential Role of NAP in Neuroprotection and in Preventing Developmental Toxicity

Prevention of ethanol toxicity in mouse embryos by NAP and SAL could be a result of their neuroprotective activity or from their ability to antagonize ethanol inhibition of L1-mediated cell adhesion (ethanol antagonism). To determine the role of ethanol antagonism and neuroprotection in NAP prevention of ethanol embryotoxicity, we performed an Ala scanning substitution of the NAP peptide [125]. The Ser-Ile-Pro region of NAP was crucial for both ethanol antagonism and protection of cortical neurons from tetrodotoxin (neuroprotection). Ala replacement of either Ser-5 or Pro-7 abolished NAP neuroprotection, but had relatively minor effects on the efficacy of NAP antagonism of ethanol. In contrast, Ala replacement of Ile-6 (I6A-NAP) caused only a small reduction in the efficacy of NAP neuroprotection, but markedly reduced the efficacy (50%) and the potency (5 log orders) of ethanol antagonism (see Table 2).

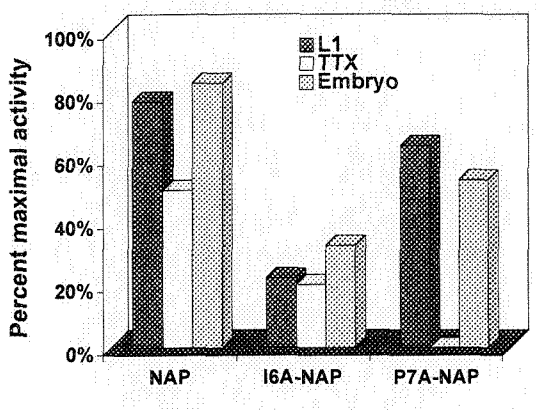

Figure 10. Relative effect of NAP mutants on ethanol antagonism, neuroprotection, and prevention of ethanol teratogenesis. Data for 10 pM of the indicated peptides are expressed as a percentage of maximal NAP effect (ethanol antagonism, neuroprotection) or as a percentage of maximal possible prevention ethanol teratogenesis. "L1" refers to percentage of maximal NAP antagonism of ethanol inhibition of L1 adhesion; "TTX" indicates percent of maximal NAP protection of TTX neurotoxicity; "embryo" refers to the percentage of peptide protection from the full reduction in somite number caused by ethanol. A different measure was used in the whole embryo experiments, because it was not feasible to establish a maximal NAP effect through a dose response

Ethanol significantly reduced the number of paired somites in mouse whole embryo culture. This effect was prevented by co-incubation with 100 pM NAP or 100 pM P7A-NAP, but not by 100 pM I6A-NAP (Figure 9 A and B). Therefore, the structure activity relation for NAP prevention of ethanol-induced embryotoxicity was similar to that for ethanol antagonism and different than that for NAP neuroprotection (Figure 10) [125]. These findings support the hypothesis that antagonism of ethanol inhibition of L1-mediated cell adhesion by NAP plays a central role in the prevention of ethanol toxicity by NAP.

Photolabeling Alcohol Binding Sites on L1: New Studies

These results highlight the importance of ethanol effects on L1 function in the pathophysiology of FASD and the potential for the development of agents that block ethanol toxicity. Therefore, identifying the binding sites for ethanol (agonist) and 1-octanol (antagonist) would be important steps in the design of more rationale antagonists. Our working hypothesis for this proposal is that these binding sites occur on L1. We will therefore use purified L1, photoactive derivatives of butanol and octanol (azibutanol and azioctanol, respectively) and mass spectrometry to identify these binding sites. The sections below describe our preliminary data using azialcohols as photoactive ligands, the activity of the azialcohols as agonists and antagonists for L1-mediated cell adhesion and the purification of the target molecule L1.

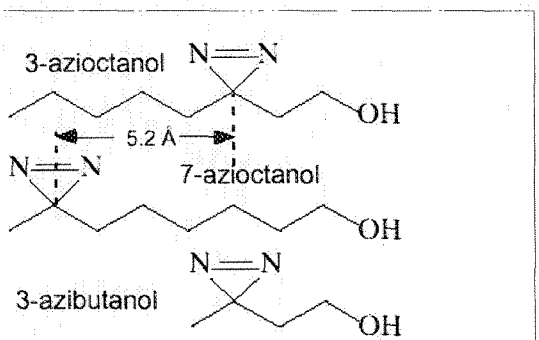

Figure 11. The Azialcohols for use in this proposal. Photoreactive alcohols for locating antagonist and agonist binding sites.

Photoactivable Alcohols Behave Like Normal Alcohols

Ideally for this project one would like a photolabel that was a derivative of ethanol. However, for stability there needs to be two carbons between the diazirine and hydroxyl groups and no hydrogen on the same carbon as the diazirine, so the smallest stable diazirine–bearing alcohol is a butanol derivative, 3-azibutanol (Figure 11). Like butanol, it is a general anesthetic *in vivo* (EC50 = 24 mM) and enhances GABA–induced inhibitory currents. It inhibits acetylcholine–induced excitatory currents (IC50 ~ 40 μM) elicited by high AcCho concentrations, but enhances those elicited at low AcCho concentrations because it shifts the AcCho concentration-response curve to the left while lowering its maximum (Forman & Miller, unpublished data). All these actions are remarkably similar to butanol's, including inhibition of L1-mediated cell adhesion (see below).

Photoactivable Alcohols: Identification of Binding Sites on Adenylate Kinase

Our first study using 3-azioctanol on the nAcChoR used classical amino acid sequencing techniques for identifying the alcohol sites [113] (see Appendix). This had the disadvantage of requiring tritiated 3-azioctanol and large amounts of protein. We have subsequently introduced the use of mass spectrometry for identifying drug binding sites on proteins. This dramatically reduces the amount of protein required and eliminates the need for radiolabeled alcohols, except in the initial reconnaissance phase of the project when they are needed both to identify photolabeled proteins and to guide the development of methods to purify fragments of such proteins. Mass spectrometry accurately measures the charge–to–mass ratio (m/z) of peptides and proteins from molecular weights of 500 Da up to about 30 kDa, thus yielding the number of photoincorporated alcohols in a single experiment. With peptides a protocol termed MS/MS can select a single peptide from a mixture based on m/z, and then by colliding it with inert gas atoms cause fragmentation at peptide bonds allowing the peptide to be sequenced. This method is currently applicable in the 0.5-3 kDa range (~3 to 24 amino acid residues) [126]. This experiment often allows the single amino acid residue with the photoincorporated alcohol to be identified. We have successfully identified alcohol binding sites both on adenylate kinase [127, 128] and on expressed fragments of PKC [129] that contain diacylglycerol binding sites (see below). The alcohol–containing proteolytic fragments sequenced in these studies contained 13 and 22 residues respectively.

Our completed study of adenylate kinase [127, 128] illustrates the power of the method and defines the experimental strategy to be utilized in this proposal. We chose adenylate kinase, which is known to interact with volatile general anesthetics [130], because its structure is well characterized [131], allowing us to interpret the results in detail. This has allowed us to verify that the methodology is reliable. Photoincorporation of [^{3}H]3-azioctanol into adenylate kinase occurred in a saturable manner with an EC50 of 180 μM, comparable to its anesthetic concentration. Adenylate kinase photolabeled with either 100 μM 3-azioctanol or 7-azioctanol was analyzed by microcapillary liquid chromatography coupled to an ion trap mass spectrometer with electrospray ionization. For both alcohols the charge envelopes for the unlabeled and labeled adenylate kinase were deconvoluted to yield molecular weights of 21,596 Da and 21,724 Da, respectively. The difference between these two molecular weights is 128 Da, which is the expected mass shift for photoincorporation of a single azioctanol molecule (Figure 12).

The stoichiometry of 3-azioctanol photolabeling, even at 1 mM, remains at 1:1, indicating there is no nonspecific photoincorporation. Adenylate kinase was photolabeled

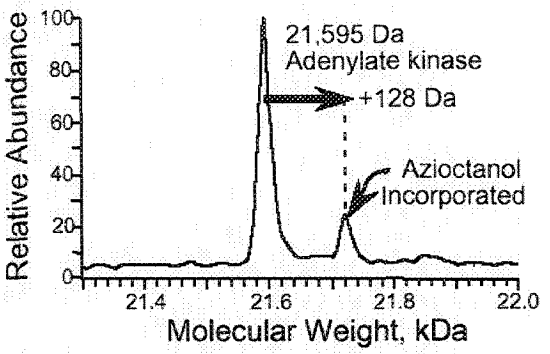

Figure 12. Photoincorporation of 3-azioctanol into adenylate kinase by LC/MS. Adenylate kinase photolabeled with 100 uM 3-azioctanol was eluted from the online microcapillary column with a gradient of 0–80% acetonitrile in 15 minutes at a flow rate of 0.6 mL/min. Mass spectra were acquired from m/z 300 to m/z 2000. The charge envelope eluting between 13.1 and 15.1 minutes was deconvoluted to yield peaks of molecular weight at 21,595 and 21,724 Da, corresponding to adenylate kinase without and with a single photoincorporated azioctanol (MW 128).

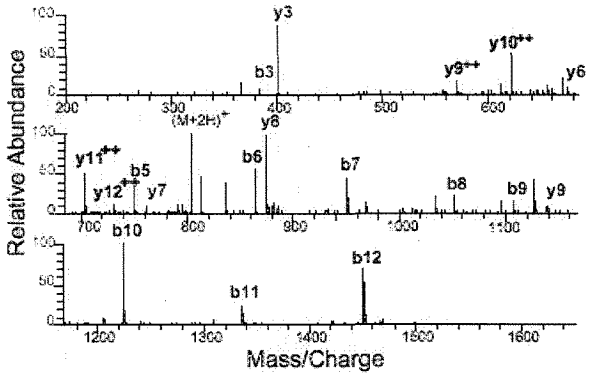

Figure 13. Identification of His-36 as the site for 3-azioctanol by LC/MS/MS. The amino acid sequence YGYTHLSTGDLLR and the site of attachment for 3-azioctanol was deduced from this spectrum. See Table3.

in parallel with tritiated and non-tritiated 3-azioctanol, digested with trypsin and fractionated by reverse-phase HPLC. A single fraction with covalently attached tritium was found. The equivalent peptide fraction from the nonradioactive sample was then analyzed by mass spectrometry. It contained a dominant peptide of molecular weight 1,623 Da, consistent with an expected trypsin cleavage product with sequence YGYTHLSTGDLLR (1495 Da) with 3-azioctanol photoincorporated (128 Da). This peptide was sequenced using microcapillary on–line liquid chromatography coupled to our ion trap mass spectrometer with electrospray ionization. The eluted peptide, in its ionized form, underwent a collision-

activated dissociation process in which the peptide randomly fragmented at the peptide bond, resulting in several smaller observed ion fragments. In this type of experiment, two series of peptide fragments are observed: ions containing the N-terminus are called "b" ions and those containing the C-terminus of the peptide are called "y" ions (Table 3). Figure 13 shows the collision-activated dissociation mass spectrum of the 1,623 Da peptide. All b-ions from 13 –> 5 have azioctanol photoincorporated but b3 has not. B4 is not observed so the incorporation site is b5 (His) or b4 (Gly: see Table 3). Y-ions from 13 –> 9 have azioctanol photoincorporated (y10 –> 12 are observed in the doubly charged form), while a strong signal comes from y8 without azioctanol photoincorporated. Thus, the site of 3-azioctanol photoincorporation is at His-36.

Table 3

Sequence	Name of Ion	Expected (Mass/Charge)	
		Un-labeled	Photo-labeled
B–Ions. Observed are in bold			
YGYTHLSTGDLLR	**B13**	1496	**1624**
YGYTHLSTGDLL	**B12**	1322	**1450**
YGYTHLSTGDL	**B11**	1209	**1337**
YGYTHLSTGD	**B10**	1095	**1223**
YGYTHLSTG	**B9**	980	**1108**
YGYTHLST	**B8**	923	**1051**
YGYTHLS	**B7**	822	**950**
YGYTHL	**B6**	735	**863**
YGYT**H**	**B5**	622	**750**
YGY**T**	B4	485	613
YGY	**B3**	**384**	512
YG	B2	221	349
Y	B1	164	292
Y–Ions. Observed are in bold			
YGYTHLSTGDLLR	**Y13**	1496	**1624**
GYTHLSTGDLLR	**Y12**	1333	**1461**
YTHLSTGDLLR	**Y11**	1276	**1404**
THLSTGDLLR	**Y10**	1113	**1241**
HLSTGDLLR	**Y9**	1012	**1140**
LSTGDLLR	**Y8**	**874**	1002
STGDLLR	Y7	761	889
TGDLLR	**Y6**	**674**	802
GDLLR	Y5	573	701
DLLR	Y4	516	644
LLR	**Y3**	**401**	529
LR	**Y2**	**288**	416
R	Y1	175	303

We recently synthesized 7-azioctanol, which, when used with 3-azioctanol, provides an isosteric pair of octanol derivatives that allow a more complete mapping of the topology of drug sites [128]. Employment of 7-azioctanol yielded Asp-41 as the site of photoincorporation [128]. Thus, the strategy of placing diazirine groups on both the 3- and 7-positions of octanol was remarkably successful, leading to the identification of two amino acids separated by four residues. The maximum distance between the third and seventh carbons of a fully extended aliphatic chain is 5.2 Å (Figure 14). Inspection of the crystal structure of adenylate kinase shows the distance between the α–carbons of His-36 and Asp-41 to be about 10 Å and the closest approach of their side chains to be ~5Å, suggesting that the octanol chain binds in a mostly extended conformation with the its third carbon near His-36 and its seventh carbon near Asp-41 [132]. These two amino acids are on different domains of the protein and when substrate is bound the two residues rotate relative to each other around Ser-38 changing the geometry of the site [133] and altering photoincorporation of azioctanol (unpublished data). In a comparable study of PKC, both alcohols photoincorporated into the same residue, suggesting that octanol binds this site in a coiled conformation.

The PKC study was designed to test the hypothesis of Stubbs and colleagues [11] that alcohols act on this protein by interacting with only one of the two diacylglycerol sites. We expressed each of these sites and found we could only photolabel one, thus confirming the hypothesis [129]. These examples serve to emphasize the power of these recently introduced methods.

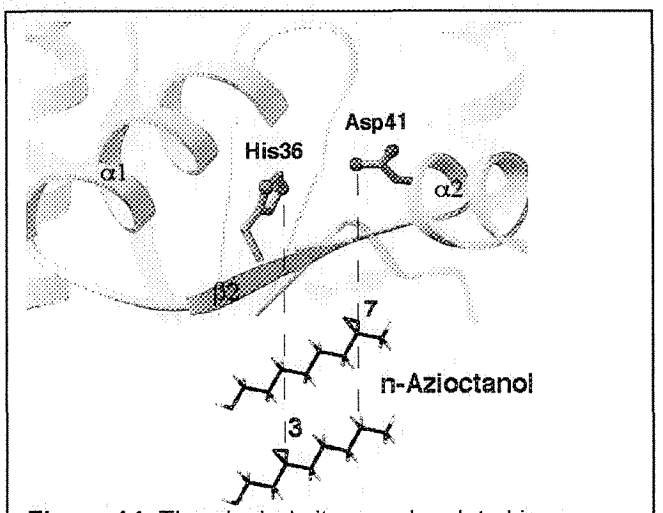

Figure 14. The alcohol site on adenylate kinase, showing the relationship between the position of the diazirine group on the octanol backbone and the amino acid residues they photolabel. Octanol's hydroxyl is to the left.

Azialcohols Mimic Their Parent Compounds With Respect to Agonist and Antagonist Activity

Before attempting to photolabel L1 we wanted to demonstrate that the diazirine-modified compounds retain the pharmacological properties of the parent compounds. We therefore compared the ability of 3-azibutanol to inhibit L1-mediated cell adhesion against its parent molecule 1-butanol, using our 2A2-L1 cell line. Single aqueous concentrations were chosen to produce

a molar membrane concentration equivalent to that produced by a buffer solution of 100 mM ethanol. This concentration of ethanol maximally inhibits L1-mediated cell adhesion and is still physiologically relevant [124]. As shown in Figure 15, 3-azibutanol proved almost as effective as an inhibitor of L1-mediated cell adhesion as 1-butanol. Cell adhesion in control cells was 41.7 ± 1.6%, while 6 mM 1-butanol and 3-azibutanol decreased cell adhesion to 27 ± 1% (n=3) and 31 ± 2% (n=4), respectively ($p<0.001$). Cell viability was unaffected by either alcohol treatment, as judged by Trypan blue staining (data not shown).

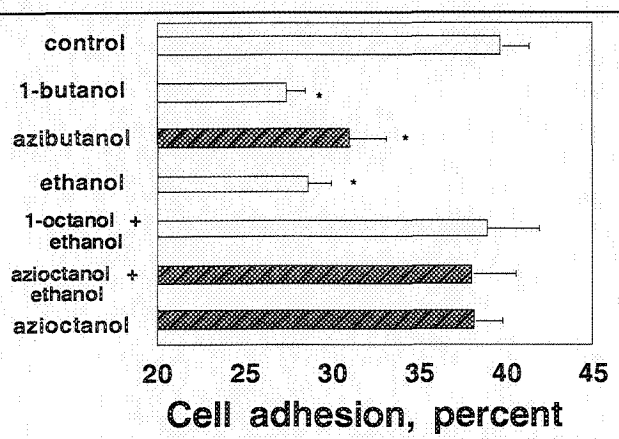

Figure 15. Azialcohols behave like the parent alcohols on cell adhesion. Cell adhesion assays were performed with 2A2-L1 cells in the absence (control) and presence of the indicated alcohols. Bars represent the mean percentage ± SEM for cell adhesion from 3 to 5 experiments. 1-butanol (6mM), 3-azibutanol (11mM), ethanol (100mM), 1-octanol + ETOH (50μM/100mM), 3-azioctanol + ethanol (14μM/100mM), 3-azioctanol (14μM). (*) Cell adhesion in the presence of 100 mM ethanol (28.5 ± 2, n=4), 6 mM 1-butanol (27±1.1, n=3) and 3-azibutanol (31±2.1, n=4) was significantly less than with control cells (41.71.6, n=4) (paired t test, t = 9.4, 13.5, 12.3 respectively; $p<0.001$).

Similarly, we compared the antagonist properties of 3-azioctanol to its parent alcohol, 1-octanol, again using our 2A2-L1 cell line. 1-Octanol (50 μM) almost completely blocked ethanol (100mM) inhibition of L1-mediated cell adhesion (Figure 15). Due to limited quantities, the maximum concentration tested was 14 μM 3-azioctanol. Added to the cells alone 3-azioctanol had no effect on cell viability, nor did it significantly change L1-mediated cell adhesion (control = 40 ± 2%, 3-azioctanol = 38.2 ± 1.7%, $p>0.2$, n=5). Figure 13 shows that 3-azioctanol was a very effective antagonist of ethanol inhibition of cell adhesion. Ethanol (100mM) alone reduced cell adhesion from control levels of 40 ± 2% to 28 ± 1.5% (n=5). However, in the presence of 3-azioctanol (14 μM) plus 100 mM ethanol cell adhesion was not different than control samples (38 ± 2% and 40 ± 2%, respectively, n=5). These data suggest that each azialcohol is as potent and has similar pharmacological properties as the parent alcohol, with respect to their effects on L1 cell adhesion. Further pharmacological characterizations are described in section D, below.

Affinity Purification of Target Molecule, L1

An important procedure required for the proposed experiments is the affinity purification of L1. We have succeeded in doing this using a modified protocol, first established by Wolff and colleagues [134]. Cell extracts were prepared from 2A2-L1 (NIH/3T3 cells transfected with human L1 cDNA) using NP40 extraction buffer and protease inhibitors (see Methods, for details). The extract was incubated with anti-L1 polyclonal (SC1508, Santa Cruz) antibody attached to agarose beads (Seize X kit, Pierce) and eluted with low pH buffer. Purity was checked by SDS-PAGE and immunoblotting. Figure 16 shows a representative immunoblot of affinity purified L1 from 500 ug of cell extract. Only two immunopositive bands are visible, corresponding to the 210 and 190 kDa bands of L1 normally found from our transfected cells [54, 93] and others [135]. Silver staining revealed the presence of a prominent band at 210 kDa and lesser amounts of smaller molecular mass proteins (between 180 and 100 kDa) (lanes 4 & 5, Figure 16). Extracts from vector transfected cells had no immunoreactive bands after western staining (Figure 16, lane 3) or detectable protein with silver staining (Figure 16 lane 6). For further purity we will repeat the affinity purification scheme or use HPLC with a C4 column.

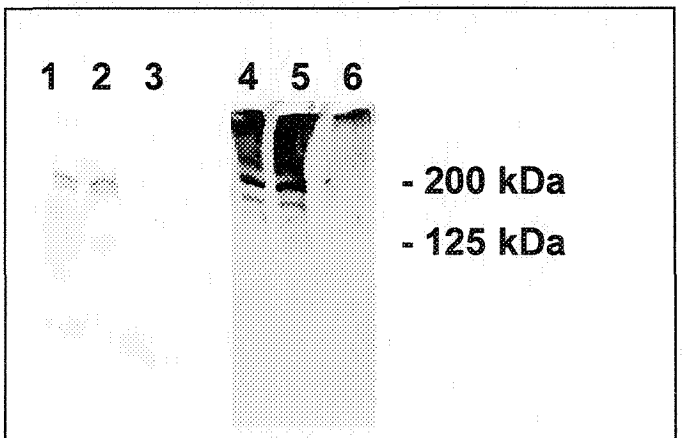

Figure 16. Affinity purification of L1. Cell extracts from 2A2-L1 cells (lanes 1,2,4,5) or vector (lanes 3,6) were mixed with an anti-L1 affinity column (rabbit anti-L1 antibody (SC1508) attached to agarose beads) and eluted with low pH. Elutions were separated by SDS-PAGE and immunoblotted (lanes 1-3) or silver stained (lanes 4-6). Only the 2A2-L1 cell extract had immunoreactive L1 bands at 210 and 190 kDa. See text for further details.

D. EXPERIMENTAL DESIGN AND METHODS

Overview: Photolabeling of alcohol sites

The overall strategy for characterizing agonist and antagonist sites on L1 is very similar and they can be considered together. Initially, L1 will be photolabeled with an agonist, [^{3}H]3-azibutanol, or an antagonist, [^{3}H]3-azioctanol. The location of the sites of labeling will then be narrowed down by degradation of L1 into smaller fragments.

The pharmacology of photoincorporation into these fragments will be used to characterize the nature of the sites. For example, the concentration–dependence of photoincorporation into saturable sites will be compared to the cellular pharmacology of the azialcohols, with respect to L1-mediated cell adhesion.

Finally, at pharmacologically relevant sites the amino acids that are photolabeled will be determined. In the case of the antagonist site, 7-azioctanol will be used to further define the binding locus.

The methods for implementing these strategies and the interpretation of results are described below.

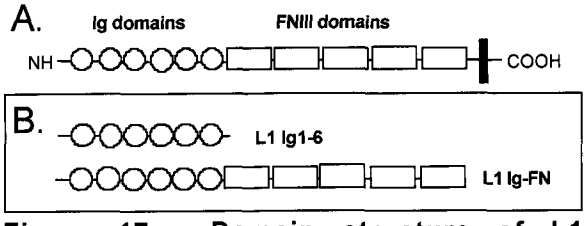

Figure 17. Domain structure of L1 polypeptide. A. The cartoon schematic shows the modular array of the extracellular domains of L1. Ovals represent the I-set immunoglobulin (Ig) domains 1-6, and rectangles represent the five fibronectin type III-like (FNIII) domains. The transmembrane region is shown as a vertical bar. The cytoplasmic region is shown as a line following the transmembrane region, ending at the carboxy terminus. The domains are not to scale. **B.** Shown in the box are the polypeptide fragments of L1 that will be used first for photolabeling with the azialcohols.

1. Labeling of Intact L1 with azialcohols

1.1 Choice of target molecules

The most straightforward mechanism to explain ethanol inhibition of L1-mediated cell adhesion is direct binding of ethanol to L1 at or near the region required for cell adhesion. A cartoon schematic of the domain structure of L1 is shown in Figure 17. The molecular mechanism underlying L1–mediated cell adhesion is thought to involve direct interaction of a portion of the extracellular region, including the first 6 immunoglobulin domains (Ig1-6) (see Background and reviewed in [66, 136, 137]). Therefore, our strategy will be to start by photolabeling the part of L1 most likely involved in alcohol action, and then to proceed in two steps to the intact protein. All of the L1 molecules used in these studies will be human in origin.

1.1.a Truncated L1 (L1 Ig1-6): We will start with a truncated L1 polypeptide, containing only the first Ig domains (L1-Ig1-6 in Figure 17). We obtained this polypeptide from the laboratory of Dr. Martin Grumet (see letter of collaboration), who has done extensive work on the purification of L1 and related cell adhesion molecules [74, 138, 139]. This polypeptide retains the same neurite outgrowth promoting activity as intact L1 [139].

1.1.b. Entire extracellular region (L1 Ig-FNIII): We will then proceed to photolabel a human L1 polypeptide containing the entire extracellular region (domains Ig1-6 and FNIII 1-5, see Figure 17). Even if there is both an antagonist and an agonist site on the L1Ig1–6 polypeptide, additional sites may occur either within the FNIII domains or at the junction of the Ig and FNIII domains or at a pocket created by the contact of two non-contiguous domains. This polypeptide will be isolated by Dr. Wilkemeyer's laboratory from cell lines expressing the human L1 Ig-FNIII polypeptide as an Fc chimeric protein. These cell lines will be obtained from Dr. Grumet [139, 140] or from Dr. Cynthia Bearer [94]. This fragment of L1 also retains biological activity [94, 139, 140]

1.1.c. Full length intact human L1: Finally, for the same reasons outlined above. we will examine the intact human L1 molecule, which we can isolate from our transfected cell line, 2A2-L1, by scaling-up the affinity purification described above and in Methods.

1.2 Purification strategy

The first step in these experiments is to obtain sufficient quantities (1-3 mg) of >90% pure proteins. Such samples will ensure the feasibility and efficiency of the photolabeling. However, because of the sensitivity and resolving power of mass spectrometry sites can be identified with smaller less pure samples. Larger quantities will, however, be necessary for characterizing the pharmacology of sites (Section 1.3).

1.2.a. Truncated L1 (L1 Ig1-6): Using a novel expression vector containing a human L1-Fc chimeric protein, Dr.Grumet's laboratory has purified >10 mg of this polypeptide [74, 139] and he has agreed to provide us with at least 1-2 mg for photolabeling (see collaboration letter). The purification strategy used for this polypeptide is outlined in the Methods section and in Haspel et al, 2001 [139].

1.2.b. Entire extracellular region (L1 Ig-FNIII): For the entire extracellular region of human L1 (L1 Ig-FN in Figure 17) we have two sources, the laboratories of Dr. Martin Grumet or Dr. Cynthia Bearer (both have

submitted letters of collaboration agreement). Both laboratories have agreed to supply us with the cell lines transfected with an L1-Fc chimera. Dr. Wilkemeyer's laboratory will grow the cells and isolate the L1 polypeptide as described in the Methods section. Briefly, soluble proteins (including the L1-Fc polypeptide) from the culture media are concentrated with ammonium sulfate precipitation and the L1-Fc polypeptide is purified using DE52 columns followed by affinity chromatography using protein A sepharose beads.

1.2.c. Full length L1: Full length intact human L1 will be isolated from our L1-transfected cell lines (2A2-L1). We have successfully purified L1 using immunoprecipitation (Figure 16). We will refine and scale up this method to produce milligram quantities of L1. We estimate that this will require growing and harvesting L1–producing cells from approximately 200 T75 flasks (see Methods). Working in collaboration with the protein chemists in Dr. Miller's laboratory, we will design further purification protocols using HPLC with C4 or C18 columns to obtain >90% purity. Protein purity will again be confirmed by SDS-PAGE and L1 immunoblotting. Because the photolabeling of this protein will be tackled towards the end of the project, we will have time to develop the expression and purification methodologies. As noted in the introduction to this section, good progress on some aspects of this project can be made with amounts of intact L1 that are readily achievable earlier in the project.

2. Labeling of L1

Based on our experience with nAcChoR and adenylate kinase A, a mixture of L1 (~100 μM; 50 μL) and [^{3}H]3-azioctanol (1 – 100 μM) will be pre-incubated for 10 minutes and then exposed for 15 minutes to UV irradiation at 365 nm at a distance of 2 cm with a model UVL-56 20 W Blak-Ray handheld lamp (Upland, CA). A control sample will be prepared without UV irradiation. Protein concentration will be varied depending on the use for the sample (mass spec needs ~nmoles or less, protein chemistry much more) and losses during proteolysis and purification. The choice of ligand concentration is related to potency but also subject to experimental design considerations discussed below.

2.1.a Strategies for finding sites of photoincorporation - Initial stoichiometry.

The extracellular 1101 amino acids of L1 have a molecular weight of 123,186 Da and runs from the end of the signal peptide (Ile20) to the end of the fifth fibronectin domain (Glu1121; Figure 18). Photolabeling with azialcohols will be carried out as described ([141] and Methods). The photolabeled protein will be chemically digested with hydroxylamine (NH_2OH, 2 M) under reducing conditions in the presence of 4 M guanidinium hydrochloride at pH 9. This cleaves the peptide bond at asparagine residues and is expected to yield 7 polypeptides with molecular weights ranging from 1.5 to 47 KDa. Initially, peptides carrying the photoincorporated ligand will be identified using gel electrophoresis techniques (SDS-PAGE) followed by high performance liquid chromatography (HPLC). Coomassie blue stained SDS-PAGE bands will be cut from the gel and the radioactivity determined by scintillation counting. Subsequently, HPLC purification of the cleavage fragments will be carried out using a C18 column, 300 Å pore, 5 um particle size, dimensions 4.6 mm x 250 mm. If unexpectedly strong hydrophobic interactions between some peptides and the column occur, a less hydrophobic column, such as a C4, will be utilized. The conditions of the mobile phase in the HPLC will be optimized in order to efficiently separate the polypeptide fragments. Elution of the fragments will be monitored at 210 nm. Continuous 1 ml fractions will be collected and scintillation–counted to identify the fractions containing tritium. Peptides will be identified by their molecular weights determined by LC/MS (see below for details).

Table 4

Residue # in the Soluble L1 sequence	Molecular Weight (in daltons)	Domain
1-171	19,390	Ig1-Ig2
172-350	20,192	Ig2-Ig3-Ig4
351-460	12,226	Ig4-Ig5
461-880	46,964	Ig5-Ig6-FNIII (1-3)
881-926	4,937	FNIII (3-4)
927-1086	17,980	FNIII (4-5)
1087-1101	1,528	FNIII 5

The initial focus will be on the first 6 immunoglobulin domains given the extensive data showing the importance of this region in hemophilic interactions.

2.1.b Strategy for the 46,964 Da (47 kDa) proteolytic fragment of L1: In case the 47 kDa polypeptide fragment of L1 (Table 4) is labeled with the azialcohol, the peptide will be subsequently cleaved with CNBr in order to generate 5 smaller fragments that can be separated and identified in a manner similar to that outlined above. This strategy is illustrated in Figure 18.

Interpretation and expected findings: Tritium incorporation will identify which fragments of L1 contain photoincorporated azioctanol. LC/MS of the parallel purified nonradiolabeled samples will yield the stoichiometry of photoincorporation. This defines how many sites of photoincorporation will be sought in the next phase. If very high stoichiometries of photoincorporation are encountered, then further digestion of such peptides will be made. In difficult cases, we will repeat labeling with lower concentrations of azioctanol in order to label only the sites of highest

affinity. For example In the case of the nAcChoR we used concentrations as low as 1 uM. Pharmacological

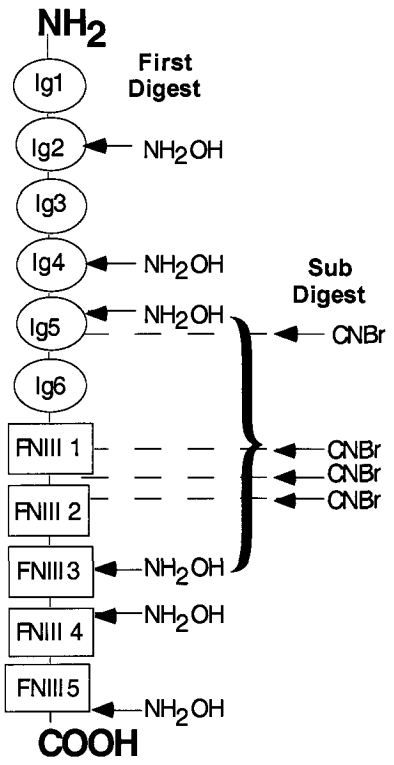

Figure 18. Domain structure of human L1 polypeptide with cleavage sites for its digestion by hydroxylamine (NH_2OH) and subdigestion of the largest NH_2OH fragment by cyanagen bromide. (CNBr).

characterization of photoincorporation sites identified above is considered in section 1.3 below.

Because there may be other sites, the full sequence of L1 will also be examined including the transmembrane region and the intracellular C-terminal. For this strategy we will use L1 purified from the transfected fibroblasts or purified from rodent brain. The overall approach will be the same, but the cleavage pattern produced with hydroxylamine will be re-evaluated.

2.2 Strategies for finding photoincorporation sites

The identified labeled peptides will be subdigested with trypsin, which usually provides cleaved peptides with the appropriate charge for mass spectrometry. (Samples will be added to solutions containing 100 mM ammonium bicarbonate to a final volume of 300 μL and digested overnight at room temperature with trypsin at a ratio of 1:35 protease:protein. The digested samples will be stored at –20°C until needed for analysis). The subdigested peptides will be subjected again to LC/MS and LC/MS/MS in order to precisely determine the location of the alcohol.

2.2.a. Identification of sites by mass spectrometry: Mass spectral data acquisition will be performed by LC/MS and LC/MS/MS on an ion trap mass spectrometer equipped with a custom-built nano-electrospray ionization source (LCQ, Finnigan MAT, San Jose, CA). Parallel non-tritiated fractions will be concentrated and then screened by online LC/MS/MS using a 75 mm x 360 mm microcapillary column packed with POROS reverse phase material. The column will be connected to a 5 μm ID fused silica tip via a zero dead volume union. One mL of each concentrated fraction will be loaded onto the column and peptides will be eluted with a gradient of 5-65% acetonitrile/0.1 M acetic acid for 60 minutes, followed by 65-80% acetonitrile/0.1 M acetic acid for 10 minutes. Mass spectra will be acquired continuously with time from m/z 300 to m/z 2000 with automatic gain control. (Alternatively, an aliquot of the digest reaction mixture can be analyzed directly by online LC/MS/MS.) The ion trap mass spectrometer will be acquiring both molecular weight information (MS scans) as well as sequencing information (MS/MS scans). The MS/MS spectra will be acquired initially with data-dependent acquisition of the most intense ion from each MS scan, but, depending on results, the control software can be set to acquire a specific peptide identified as being modified by an azialcohol or to acquire up to the six most abundant ions. We will use the database-searching algorithm SEQUEST, to assist in the identification of labeled and unlabeled peptides derived from the digests. We will locate the modified amino acid by identifying the ions that contain the appropriate mass shift. Typical data have been shown in Section C. Although the MS generates a huge amount of data, it comes with powerful software that automates much of the analysis.

Interpretation and expected findings:

Typical mass spectrometry data and their interpretation have been considered in Section C. The work on L1 will be evaluated similarly. It is our experience that not all predicted peptide sequences in a digest are found. This might be because some fragments consist of only one or two amino acid residues (too small to be detected by the mass spectrometer), because the chromatography is not optimal, or because ionization does not occur (this depends on the component amino acids of the peptide which must bear at least one net positive charge to be analyzed). In many cases the best strategy is to modify the digestion procedure to produce different fragments. A large variety of proteases and standard chemical techniques are available. The choice would be made depending on the particular sequence under consideration (see for example Pratt et al in the Appendix [142]). If chromatography is the issue, conditions will be varied (replace the C18 column by C4, C8 or hydrophilic interaction columns, modify the solvent gradients).

3. Pharmacological characterization of photoincorporation sites:

Introduction:

It seems likely for a number of reasons that we may find more than one alcohol site.

i. The pharmacology of cell adhesion, summarized in sections B and C, suggests that separate sites for azibutanol (an agonist) and azioctanol (a noncompetitive antagonist—this assumes it behaves like octanol, an assumption we will test) will be found on L1. Because alcohols act at relatively low affinity, there may be cross talk between these sites. For example, an agonist might interact with the antagonist site but with much lower affinity than at the agonist site.

ii. The molecular weight of L1 is ~145 kDa (before glycosylation) and because it presents a large target to alcohols it would not be surprising to find more than one site of interaction. Indeed in adenylate kinase, which has a molecular weight of only 21,595 Da, we found there were two sites for 3-azibutanol but that only one of these bound 3-azioctanol, so the assumption of separate sites has some validity. Inspection of the known structure of adenylate kinase, revealed the reason for this. The site that only bound 3-azibutanol was too small to accommodate 3-azioctanol.

iii. Nonspecific binding sites are to be expected because the low affinity with which alcohols act means that high concentrations are employed leading to enhanced nonspecific binding.

iv. The structure of L1 contains six I-set Ig domains and five S-set domains (fibronectin type III-like; FNIII) which likely share some structural features, including possibly alcohol binding sites.

Thus, we need to set up criteria for distinguishing which of the several expected photoincorporation sites are saturable and pharmacologically relevant.

3.1. Distinguishing saturable sites from nonspecific sites of photoincorporation

A priori we expect to encounter two different types of binding site. First, discrete saturable sites whose occupancy follows a binding isotherm. Second, nonspecific sites whose occupancy depends linearly on the free alcohol concentration. To distinguish the two types of photoincorporation we will photolabel L1 at a series of concentrations of azialcohol. The free concentration will be known, and the degree of photoincorporation can best be measured by HPLC of the appropriate digest fraction. HPLC monitors both the protein concentration (absorbance at 210 nm) and the cpm in the corresponding fraction collected.

Note that mass spectrometry is not optimal for measuring the degree of photoincorporation because there is no independent method of verifying how much peptide reached the ionization chamber or was actually ionized.

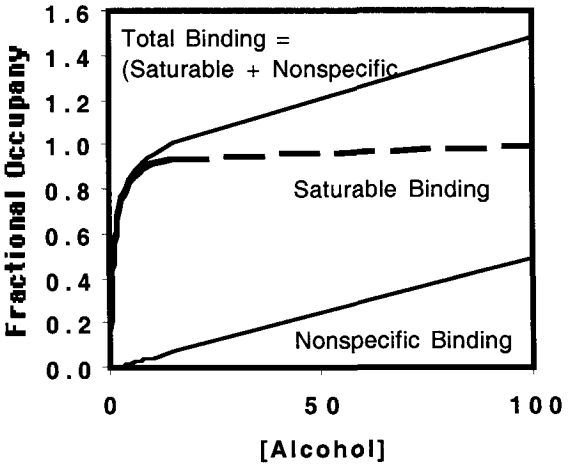

Figure 19. Expected behavior for binding consisting of both saturable binding to a site and nonspecific binding.

Three behaviors might be expected (Figure 19). Only saturable binding, only nonspecific binding, and a combination of the two. A forth possibility arises if there are two saturable sites. If these are noninteracting and their dissociation constants not too dissimilar, saturable binding will be observed with a Hill coefficient that is less than one because of the unresolved overlap of two saturable curves. Hill coefficients greater than one can result from interacting sites, but it is unlikely the methods employed will be of sufficient accuracy to determine such subtle changes.

3.1.a. Mitigation of nonspecific binding

Based on our experience to date, azialcohols tend not to photoincorporate nonspecifically at high levels. If such a situation should arise, however, we can decrease the fraction of nonspecific binding in a number of ways. First, we can lower the concentration of azialcohol at which we photolabel, which will increase the ratio of saturable to nonspecific photoincorporation. For example in our studies of the acetylcholine receptor we have routinely used concentrations of [^{3}H]3-azioctanol as low as 1 uM whereas with adenylate kinase at 1 mM 3-azioctanol we say negligible nonspecific binding. However, this will lower the absolute amount of photoincorporation which could be a problem in some cases. An alternative strategy would be to photolabel in the frozen state. This freezes the equilibrium state. The nonspecific surface of the protein has just a few areas in contact with alcohols, whereas in solution azialcohols continue to bombard the whole surface throughout the minutes of photolabeling.

For example, we find less labeling of the lipid-protein interface of the acetylcholine receptor under these conditions.

Overall, this issue is more likely to be a problem with the agonist, 3-azibutanol, than with the antagonist, 3-azioctanol. This is because the former's half effect concentration is approximately 10 mM whereas the latter is approximately 14 uM.

Determining if saturable sites are functional
The above studies will have provided an estimate of the apparent dissociation constant for photoincorporation at a each site characterized. Comparison of these with the values determined from functional studies on cell adhesion, will provide the first information on which are likely candidates as active sites.

Distinguishing agonist from antagonist sites
Any site only photolabeled by 3-azibutanol will be a candidate agonist site, whereas those photolabeled by azioctanol will be candidate antagonist sites. Some sites will be photolabeled by both agonists and antagonists. In this case only relative affinity will provide a guide.

3.1.b. Allosterism
Allosteric interactions provide the best method of categorizing which site is which. That octanol is a noncompetitive antagonist of ethanol means that it binds to a separate site which stabilizes a conformation of L1 that has weaker affinity for ethanol. By the principle of microscopic reversibility, ethanol must bind to a conformation that has weaker affinity for octanol (Section 4.8).

Allosteric interactions with 3-azioctanol
Thus, we will study photoincorporation of [^{3}H]3-azioctanol into L1 in the presence and absence of agonists shown in Fig. 1. The cleanest results will be expected for the agonists with highest apparent affinity which is 3,3-dimethyl butanol with an apparent dissociation constant of 50 uM. Thus, photolabeling will be carried out in the presence of 0, 5, 50, 500 & 5000 uM 3,3-dimethyl butanol using as low a concentration of [^{3}H]3-azioctanol as practical based on experience. The appropriate digestion and HPLC protocol will then be applied to yield the molar photoincorporation into the fragments of L1. The expected result for the antagonist site is that photoincorporation of [^{3}H]3-azioctanol will decrease in a curvilinear fashion as the occupation of the agonist site by 3,3-dimethyl butanol increases. Should competition of the two alcohols for the same site occur a linear decrease of photoincorporation would be observed. Alternatively, if no dependence of [^{3}H]3-azioctanol photoincorporation on 3,3-dimethyl butanol concentration is observed, the octanol site under consideration is not one that functions as an antagonist site for L1-mediated cell adhesion. We have considerable experience with the problem of distinguishing these three types of interaction between two alcohols binding to a single protein and have developed effective strategies [106, 143]. The equations which govern the behavior in each case are given in Section 4.8 below.

Allosteric interactions with azibutanol
The design and interpretation of the experiment is the same when [^{3}H]3-azibutanol photoincorporation into a potential agonist site is considered, but a high affinity antagonist must be substituted for 3,3-dimethyl butanol. Dodecanol and undecanol have IC50s of 10 and 30 nM respectively. We will choose undecanol because experience dictates that its lower hydrophobicity makes it significantly easier to work with. Photolabeling of L1 with, say, 1 mM [^{3}H]3-azibutanol in the presence of 0, 3, 30, 300 & 3000 nM undecanol (its saturated solubility in buffer is ~80 uM) will be carried out and analyzed as above for the agonist site. That is, the site photolabeled will only be categorized as an agonist site if photoincorporation is inhibited in a curvilinear fashion.

3.1.c. Competition with alcohols
An alternative strategy which provides a final set of criteria to categorize a site pharmacologically is competition of photoincorporation with alcohols thought to bind the same site. Thus, [^{3}H]3-azioctanol photoincorporation into a site categorized by allosteric criteria above would be competed with say undecanol. The expected result being a linear decrease of photoincorporation with increasing undecanol concentration. A control would be provided by substituting tetradecanol for undecanol because the former has no antagonist action.

Although this method has an appealing simplicity, we may encounter some difficulty as follows. These are low affinity ligands that are expected to stay on their binding sites less than a second. During photolabeling, which normally takes minutes, the azialcohol will still sample all the sites, it will just take longer because some will be transitorily occupied by another alcohol on the first visit, but on subsequent visits this will not always be the case. Simulations show that the rate of photolabeling changes but not the extent at equilibrium because the irreversible ligand always wins out over the reversible one eventually. Consistent with this prediction, our unpublished data with adenylate kinase show that even at times as short as 5 seconds competition does not reduce photolabeling. We have, however, now accumulated considerable experience in photolabeling in the frozen state. This is part of a study on interactions of azialcohols with the open channel conformation of nAcChoR using a technique we developed called time resolved photolabeling [127, 144] (Dr. Arevalo is currently using this technique). This allows us to freeze a solution in a few hundred microseconds. For the purposes of the present project, this means we can trap the system in its equilibrium state. Now, the irreversible

ligand cannot revisit sites, and the photolabeling pattern should reflect the equilibrium occupancy. Thus, it seems likely that this technique will allow us to use competition to examine the pharmacology cited above. It is confirmed that L1 survives freezing.

3.1.d. Competition with peptides
The heptapeptide, SAL, reverses the effects of ethanol on cell adhesion in a surmountable fashion (Preliminary data and [102]), suggesting it competes with ethanol. Thus, it likely occupies the agonist site. Because it acts in the picomolar range, it likely has a very slow off-rate, which will allow it to compete effectively against photoincorporation even at room temperature. The principle of the experiment and the interpretation is as above.

3.2. Delineation of antagonist photolabeled sites
Once the antagonist site has been unambiguously located using the criteria above, we will label it with 7-azioctanol in order to explore the extent of the site. The diazirine moieties on 3- and 7-azioctanol are ~5.2 Å apart. If octanol binds in an extended conformation, it is possible that a different amino acid will be photolabeled, as was the case with adenylate kinase (Figure 14). The two residues labeled in that case were on separate domains of the kinase that moved relative to each other when substrate was bound, thus providing a mechanism for the observed allosteric regulation of photoincorporation. This experiment thus has the potential to provide information on the orientation of octanol in the binding site and on the mechanism of the allosteric antagonism of ethanol's action.

4. Pharmacology of the azialcohols' actions on cell adhesion
The behavior of photoincorporation sites characterized above will be compared to the functional pharmacology of cell adhesion in order to classify them. This involves characterizing in more detail than was presented in Preliminary Results the agonist actions of 3-azibutanol and the antagonist actions of 3- and 7-azioctanol. This data will also allow the azialcohols to be incorporated into the published data sets for other alcohols.

One criterion for distinguishing which of the many expected photoincorporation sites are saturable and pharmacologically relevant is to compare the apparent dissociation constants for photoincorporation (see above) with the half-maximal response values of the azialcohols with respect to cell adhesion. Additional criteria for determining the relevancy of 3-azibutanol photoincorporation will be to use competition studies.

Experimental design
All of these experiments will be conducted in 2A2-L1 cells, an ethanol-sensitive L1-expressing NIH/3T3 cell line [93]. Cell adhesion assays will be conducted as described [4, 93, 102, 124] and in Methods. Briefly, cells are harvested and triturated to form a single cell suspension. Cells are mixed in the presence and absence of the various alcohol (see below) and the extent of cell aggregation determined by phase contrast microscopy. Alcohol (1-butanol or 3-azibutanol) inhibition of cell adhesion will be calculated as [100 x (1 – the ratio of L1 adhesion in the presence and absence of alcohol)]. The antagonist activity of the azioctanols will be calculated as [100 x (1 – (% inhibition cell adhesion by butanol plus azioctanol)/(% inhibition cell adhesion by butanol alone))]. We define agonists as compounds (i.e. 1-butanol) that inhibit L1 adhesion. Antagonists (i.e. 1-octanol) are compounds that alone, have no effect on L1 adhesion, but block the action of an agonist. Concentration–effect curves will be fitted to logistic curves by nonlinear least squares fitting using the program Igor (Wavemetrics) [106].

Solutions will be covered during experiments to prevent evaporation of alcohols. Their concentration will be checked by gas chromatography. Azialcohols are stable for many hours under normal room illumination.

4.1. Pharmacological characterization of 3-azibutanol
To determine the half-maximal response value for the agonist activity of 3-azibutanol we will obtain a dose response curve similar to that used for 1-butanol. A wide range of concentrations will first be examined to explore the extent of the curve and then a more focused study will be conducted. Dr. Husain can provide us with plentiful supplies of 3-azibutanol for these studies.

Because agonist EC50s contain information about both binding and coupling to response, the dissociation constant for binding cannot be extracted from them. An additional criterion is to use competitive antagonists. To assess whether SAL antagonist activity is surmountable with 3-azibutanol, and by extension whether they bind to the same or different site(s), we will initially measure SAL antagonist activity in the presence of increasing concentrations of 1-butanol (as a control for previous studies, [102, 124]) and 3-azibutanol. We will measure cell adhesion in the presence of 10^{-11} M SAL and either 0, 2, 10, 50 and 100 mM butanol or 0, 10, 50 and 100 mM 3-azibutanol (the latter are preliminary estimates). If SAL occupies the same site(s) as 3-azibutanol, then we would expect the increased concentration of 3-azibutanol would overcome the antagonist activity of SAL). To confirm surmountable behavior, a series of 3-azibutanol agonist effect curves will be determined in the presence of increasing fixed concentrations of SAL. The expected behavior is a shift to the right of the agonist concentration–effect curves of 3-azibutanol with increasing concentrations of SAL. This shift will be governed by equation 1 in Section 4.8 below.

Depending on the success of allosteric competition of [^{3}H]3-azibutanol photoincorporation by undecanol (or

dodecanol), the antagonism of 3-azibutanol's agonist action on cell–cell adhesion by undecanol (or dodecanol) will be studied following the strategy outlined for SAL above.

4.2. Pharmacological characterization of 3-azioctanol and 7-azioctanol

To determine the half-maximal response values for the antagonist activities of 3-azioctanol and 7-azioctanol, we will use a concentration–response curve similar to that used for 1-octanol in the absence and presence of 2 mM 1-butanol [4, 124]. Choice of concentration range will be based on pilot experiments as above. We already know that 3-azioctanol may be more potent than 1-octanol, because 14 μM 3-azioctanol produced the same degree of ethanol antagonism as 50 μM 1-octanol (Figure 15).

Antagonist activity with 1-octanol was non-surmountable with increasing concentrations of 1-butanol [124], which implies an allosteric interaction between the agonist and antagonist sites. We plan to carry out similar experiments with 3 and 7-azioctanol using concentrations around their half-maximal response values and a range of concentrations of 1-butanol (0 – 75 mM). If the azioctanols are interacting with the same site(s) as 1-octanol, we would predict that they too would exhibit non-surmountable antagonist activity.

We plan (see above) to use the agonist 3,3-dimethyl butanol to allosterically antagonize [^{3}H]3-azioctanol photoincorporation. Therefore, following the protocol for butanol, we will study the antagonism of this agonist by 3-azioctanol.

Depending upon its utility in photolabeling studies, 7-azioctanol will be characterized similarly.

General interpretation of results

Once the position of agonist and antagonist sites within the sequence of L1 have been determined, we will interpret the results in structural terms, first at the sequence level and then at the three dimensional level. In this discussion we will focus on the Ig domains, but a similar approach can be taken with the FN domains.

Sequence level

There are six Ig domains on L1. We will align their sequences using widely available programs and compare those domains that were photolabeled with those that were not, trying to extract some rules about what is governing binding. This strategy has worked for us in a study of PKC subdomains C1A and C1B, only one of which is photolabeled (unpublished results). Finally, we can examine alignments with other members of the Ig family to assess the probability that alcohol binding sites exist on any of them.

Another level of interpretation, more mechanistic, is too rationalize our conclusions with known models of cell adhesion. Although aspects of these models are controversial, there is agreement that the following might be involved in the mechanism of L1-mediated cell adhesion: Ig1 & 2; Ig2 & 3 in one model at least [67-71, 136], and a hinge (observed in electron microscopy) between Ig6 and FN1 [74].

Three dimensional structural level

There is a high resolution (1,8 Å) three dimensional structure of Ig1–2 of NCAM [145]. If we have agonist or antagonist sites in L1 Ig1 or 2, then we will align this sequence with NCAM's, which will allow us to estimate the position of the binding site at the secondary structure level. Because these authors advanced a model for cell adhesion, we may be able to form a hypothesis on how alcohols might effect adhesion.

Overall conclusion

Photolabeling will give clear answers to the following questions:

1. Are there antagonist and agonist sites on L1?
2. If so, where are they located at the primary structure level?
3. What is the pharmacological relevance of these sites.

These are crucial conceptual questions to resolve and this is the only direct method to do so because photolabeling provides the contact points between the alcohol and the target protein. This information is essential before rational drug design can be employed and clinical intervention conceived of. Site directed mutagenesis can provide some hints, but is often confounded by allosteric actions of the mutation on distant binding sites. Furthermore, L1 has over a 1,000 amino acid residues to mutate! Photolabeling sites would provide a useful useful short cut in selecting starting points for mutation.

4. METHODS

4.1 Reagents Alcohols will be purchased from Sigma-Aldrich or Fluka, all other chemicals will be purchased from Sigma, or as indicated. Peptides will be synthesized and purified by New England Peptides, Inc.

4.2 Cell Culture Transfected NIH/3T3 cells are cultured in Dulbecco's minimum Eagle medium (DMEM) (Life Technologies) supplemented with 10% normal calf serum (Intergen) and 400 μg/ml geneticin (G-418 sulfate, Life-Technologies). NG108-15 neuroblastoma x glioma cells will be cultured in serum-free, defined medium or medium supplemented with 10% Nu serum IV (Intergen). Cells will be cultured at 37°C, in an atmosphere of 90% air and 10% CO_2 [4, 93, 102, 124].

4.3 Cell Adhesion Assay Cell adhesion will be measured using a short-term aggregation assay of sub-confluent cells [4, 93, 102, 124]. Cells are detached by gentle agitation, mechanically dissociated to obtain a

single-cell suspension, and diluted in PBS supplemented with 0.1 mg/ml DNase to 250,000 cells/ml for NG108-15 cells and 350,000 cells/ml for NIH/3T3 cells. One ml of the cell suspension is added per well (4.5 cm^2) to a 12-well plate. The plates are wrapped in parafilm to prevent evaporation. Aqueous alcohol concentrations will be confirmed by gas chromatography. After addition of the alcohols the cells are mixed for 30 minutes on ice. Each well is scored for single and adherent cells in five or six microscopic fields of view, each containing 150-200 cells. The percentage of adherent cells is then calculated for each microscopic field and averaged. To calculate the magnitude of ethanol inhibition, we subtract the values for cell adhesion with the vector-transfected cells from those of the L1-transfected cells.

L1-mediated cell-cell adhesion is defined as the difference in percent of adherent cells between an L1-transfected cell lines (2A2-L1) and a vector-transfected cell line (Vec-1A5). This component of cell adhesion is fully inhibited by Fab fragments of an anti-L1 polyclonal antibody [93]. Agonists are defined as compounds that inhibit L1-mediated cell-cell adhesion. Agonist inhibition of cell adhesion is calculated as (100 x (1 – the ratio of L1-mediated cell-cell adhesion in the presence and absence of agonist)). Antagonists are defined as compounds that have no effect on L1-mediated cell-cell adhesion and block the action of agonists. Antagonist activity is calculated as (100 – (% inhibition cell adhesion by agonist plus antagonist)/(%inhibition cell adhesion by agonist)).

4.6 Protein studies:
Protocols for SDS-PAGE and immunoblots are slightly modified from [54, 93], as follows. Cells are harvested in calcium/magnesium-free PBS (0.13M NaCl, 0.003M KCl, 0.01M Na_2HPO_4, 0.002M KH_2PO_4), pelleted by centrifugation and resuspended in NP-40 lysis buffer (150 mM NaCl, 50 mM Tris, pH 8.0, 1.0 % NP-40) containing protease inhibitors (0.1 mM phenylmethylsulfonyl fluoride, aprotinin, 100 μM leupeptin, and 50 μM pepstatin). Cells are homogenized by vortexing, and insoluble material is removed by centrifugation at 16,000 x g for 30 minutes. 50-75 μg of protein extract is boiled for 5 minutes in the presence of 5x SDS-sample buffer (Sodium Dodecyl Sulfate (10%), Glycerol (50%), B-Mercaptoethanol (25%), Tris Base, pH 7.4 (100 mM), Bromophenol Blue (2 mg/100 ml), separated on a 4 - 15% polyacrylamide gel and electrophoretically transferred to Immobilon-P membranes (Millipore Corporation, Bedford, MA). The membranes are blocked with Tris-buffered saline (10 mM Tris HCl, pH 7.5, 0.9% NaCl) containing 0.1% Tween 20 (TBS-T), incubated with primary antibody (Neuro 4.1.1.3 or mab 74-5H7), washed, then incubated sequentially with biotinylated secondary antibody and avidin D-conjugated alkaline phosphatase. The immuno-reaction products are visualized with the 5-bromo-4-chloro-3-indoyl phosphate/nitroblue tetrazolium (BCIP/NBT) substrate kit (Vector).

4.6.a. Purification of L1-Fc chimera Purified human L1 polypeptide containing the first six amino terminal domains (immunoglobulin domains 1-6, L1 Ig1-6) will be supplied by Dr. Martin Grumet (see attached letter)[139]. Purity will be confirmed by HPLC. The entire extracellular region of L1 will be obtained as a L1-Fc chimeric protein. The cDNA expression vector encoding this polypeptide will be supplied by Dr. Grumet or by Dr. Cynthia Bearer, both of whom have a background working with this fragment in functional assays [74, 94, 140]. The chimeric protein will be produced in transfected NIH/3T3 cells and purified from the IgG-depleted culture medium using ammonium sulfate precipitation, DE52 column chromatography, followed by protein A conjugated agarose beads (Pierce) by Dr. Wilkemeyer's laboratory. L1 will then be separated from contaminating proteins by preparative PAGE or HPLC (in Dr. Miller's laboratory). Using the same overall strategy Grumet and colleagues purified 1-3 mg of L1-Fc per liter of culture supernatant [139]. Protein purity will be confirmed by SDS-PAGE followed by L1-immunoblotting or Silver staining.

4.6.b. Affinity purification of the full length L1 Dr. Wilkemeyer's laboratory will use a modified protocol, first established by Wolff and colleagues [134], to purify full length human L1 from our transfected cell lines. Based on our experience, we obtain approximately 1-10 ug of affinity purified L1 per T-75 flask of attached cells (from ~ 0.5mg total protein). We will therefore harvest cells from at least 200 T-75 flasks to obtain 1-2 mg of L1. Cell homogenates will be made in NP-40 lysis buffer with protease inhibitors as described above. The soluble portion of the extract is incubated with either anti-L1 polyclonal (SC1508, Santa Cruz) or monoclonal (74-5h7, Covance) antibodies attached to agarose beads (Seize X kit, Pierce). After 2 hrs hours of mixing the immunocomplex and beads are washed with excess NP-40 buffer and eluted with low pH buffer containing 0.5% NP40. If further purity is required we will repeat the affinity purification scheme or use ammonium sulfate precipitation and DE52 column chromatography before the affinity columns. Purity will be assessed by HPLC using a C4 column.

4.7 Synthesis of Azialcohols: We have described our synthesis of 3-azioctanol (Appendix and [109]). We make 3-azibutanol by the method of Church et al [146, 147]. We devised the following synthesis of 7-azioctanol. 2-hydroxytetrahydropyran was prepared as described in [148]. Hydroxy-3-octen-7-one was synthesized from 2-hydroxytetrahydropyran by Wittig reaction with phosphoniumtriphenyl-2- oxopropylide. A suspension of 2-Hydroxytetrahydropyran (3.2 g, 31.4 mmol) and phosphoniumtriphenyl-2-oxopropylide (10 g, 31.4 mmol) in anhydrous benzene (100 ml) was refluxed for 5 h and

then stirred overnight at room temp. After removing the solvent by rotary evaporation, the residue was extracted with hexane (3 x 100 ml). The combined extract was applied to a column of silica gel (70 g), equilibrated with hexane–ethylacetate (9.5: 0.5 v/v) and eluted with hexane–ethylacetate (9:1 v/v) to give Hydroxy-3-octen-7-one (2.2 g, 48% yield). TLC silica gel Rf 0.49 (hexane–ethylacetate 7:3). Anal. ($C_8H_{14}O_2$) C: calc. 67.57; found 67.25. H: calc. 9.92%; H 10.24. Hydroxyoctan-7-one was prepared by reduction of hydroxy-3-octen-7-one (1 g, 7 mmol) with hydrogen in the presence of 5% Pd-carbon (1 g) in dry ethylacetate (30 ml) for 24 h. The 7-azioctanol was synthesized in 39 % yield from hydroxyoctan-7-one essentially by the procedure described for the synthesis of 3-azioctanol [112]. The UV spectrum in dichloromethane had a λ_{max} of 348 nm, characteristic of the diazirine group [146, 147].

[^{3}H]3-azibutanol, a new compound, will be synthesized by oxidizing unlabeled azibutanol (1) to azibutyraldehyde (2) with pyridinium chlorochromate (procedure of Corey and Suggs [149]) and subsequent re-reduction of the aldehyde (2) with [^{3}H]-sodium borohydride to give [^{3}H]-Azibutanol (3) as described by Darbandi-Tonbakon et al. [150]. In the general scheme below R= CH_3.

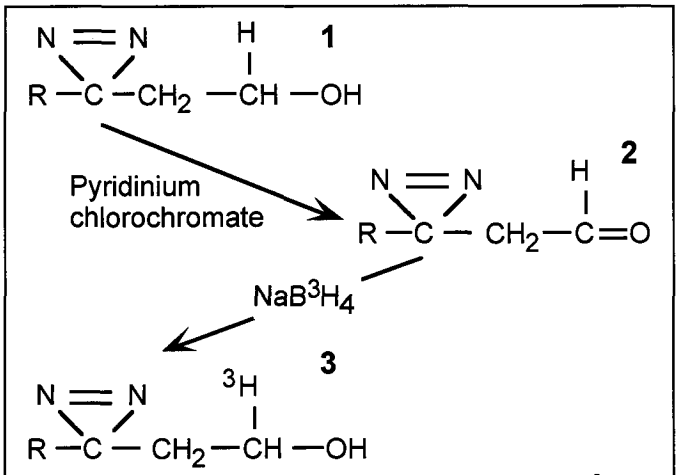

Figure 20. Proposed synthesis of [^{3}H]3-azibutanol from 3-azibutanol.

4.8 Interactions between two alcohol sites

The three types of interaction between two alcohols binding to a single protein discussed above in the Section entitled "Distinguishing agonist from antagonist sites" are governed by the relationships below.

Type 1: Unimolecular mutually exclusive binding at a single site (competitive antagonism).

When two ligands B and C bind to the same site on a protein R_O, we may write,

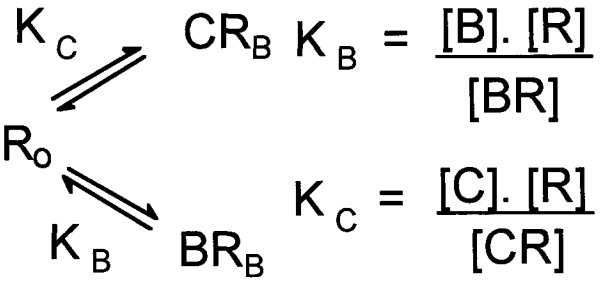

where K_B and K_C are the apparent dissociation constants for B and C respectively and BR_B and CR_B are the protein with ligand B and C bound respectively.

The presence of ligand C will increase the apparent dissociation constant of ligand B:

$$K_B^{app} = K_B(1 + \frac{[C]}{K_C}) \qquad \text{Eq. 1}$$

Thus, a plot of K_B^{app} vs. [C] will be linear with intercept K_B and slope (1/ K_C).

Type 2: Allosteric interaction at separate binding sites (for example, allosteric antagonism)

Considering the general model of ligands B and C binding to *separate* sites on protein R at individual binding sites:

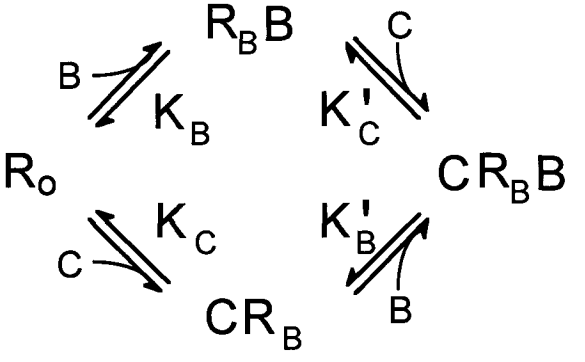

where: R_O *represents the unliganded protein*; R_BB, CR_B and CR_BB are the protein with ligands B, C, and B & C bound, respectively; K_B and K_C represent the apparent dissociation constants for B and C binding to the unliganded protein, and K_B' and K_C' represent dissociation constants for B and C binding to the monoliganded protein.

The apparent dissociation constant for B is given by:

$$K_B^{app} = K_B * \left(\frac{1 + [C]/K_C}{1 + [C]/K_C'}\right) \quad \text{Eq. 2}$$

For negative allosteric interactions (allosteric antagonism as in octanol's antagonism of ethanol's inhibition of cell adhesion), occupancy of either binding site will reduce the affinity of the other site so that $K_C' \gg K_C$ and $K_B' \gg K_B$. $K_B^{app} = K_B$ at [C] = 0 and the value of K_B^{app} increases at first linearly with low concentrations of C (because $[C]/K_C' \approx 0$).

However, as [C] becomes larger, $\left(\frac{1 + [C]/K_C}{1 + [C]/K_C'}\right)$ will deviate from linearity and eventually asymptotically approaches a constant value K_C'/K_C. Because the model demands that $\frac{K_B'}{K_B} = \frac{K_C'}{K_C}$ the asymptotic value will be K_B'.

Thus a plot of K_B^{app} versus [C] in the case of allosteric interaction will be hyperbolic. It is important to note that if $K_C' \gg K_C$ and the range of [C] used is only small - such that $[C]/K_C'$ is negligible - then the plot will appear linear because only the first part of the hyperbolic plot will be measured.

Type 3: Allosteric non-interacting binding sites
This is a special case of the above scheme in which binding of each antagonist occurs independently of the other and therefore $K_B = K_B'$ and $K_C = K_C'$. Under these conditions equation 2 reduces to $K_B^{app} = K_B$ and no shift of K_B occurs with increasing [C].

4.9 STATISTICAL ANALYSIS: All statistical comparisons will be made with an analysis of variance followed by the Student-Newman-Kuels multiple comparison of means test.

TIME FRAME FOR COMPLETION OF SPECIFIC AIMS
Sequence of research:

Protein chemistry will commence with photolabeling of purified human truncated L1 (Ig1–6) with [^{3}H]azioctanol, digestion and characterization of products on HPLC. Parallel labeling with azioctanol will allow the purified fragments to be examined by mass spectroscopy. For fragments with photoincorporation, subdigests will be developed to allow the complete sequence to be determined, thus identifying all sites of photoincorporation. This process is repeated with extracellular L1 polypeptide (Ig1 through FNIII 5) to look for additional sites on FNIII 1–5 or at domain–domain interfaces. During this process Dr. Husain will maintain supplies of 3-azioctanol and [^{3}H]3-azioctanol, and in addition synthesize de novo [^{3}H]7-azioctanol. The VA group will be characterizing the antagonist pharmacology of the azioctanols with respect to cell adhesion. In addition, they will also be working on the purification of additional L1 fragments, including the entire extracellular portion of L1 (Ig-FNIII) and the full-length L1 polypeptide. The pharmacology will enable the protein chemist to devise tests to classify the various sites of photoincorporation. The most relevant site(s) will then be studied with [^{3}H]7-azioctanol to determine the extent of the binding pocket. This is a 2-3 years work.

This cycle will be repeated with the agonist azibutanol and [^{3}H]azibutanol once Dr. Husain has synthesized [^{3}H]azibutanol. The agonist is tackled second for the practical reason that we expect to see more labeling with the lower affinity ligand. Thus, knowing which azioctanol sites are antagonist sites, will help us identify the agonist site(s).

Finally for completeness the full length L1 will be tackled to see if there are any intracellular or membrane domain sites. If these are found they will be characterized as above.

E. HUMAN SUBJECTS:

Not applicable

F. VERTEBRATE ANIMALS

None

G. REFERENCES

1. National Institute on Alcohol Abuse and Alcoholism. *State Trends in Alcohol-Related Mortality*, -., U.S. Alcohol Epidemiologic Data Reference Manual, Volume 5, First Edition. NIH Publication No. 96-4174. 1996.
2. Harwood, H., D. Fountain, and G. Livermore, The Economic Costs of Alcohol and Drug Abuse in the United States 1992. Report prepared for the National Institute on Drug Abuse and the National Institute on Alcohol Abuse and Alcoholism, National Institutes of Health, Department of Health and Human Services NIH Publication No 98-4327 Rockville, MD: National Institutes of Health, 1998.

http://www.nida.nih.gov/EconomicCosts/Table5_3.html.

3. Chen, S.-Y., M.F. Wilkemeyer, K.K. Sulik, and M.E. Charness, Octanol antagonism of ethanol teratogenesis. FASEB Journal, 2001. **15(9)**: p. 1649-1651.
4. Wilkemeyer, M.F., A.B. Sebastian, S.A. Smith, and M.E. Charness, Antagonists of alcohol inhibition of cell adhesion. Proc Natl Acad Sci (USA), 2000. **97**: p. 3690-3695.
5. Spong, C.Y., D.T. Abebe, I. Gozes, D.E. Brenneman, and J.M. Hill, Prevention of fetal demise and growth restriction in a mouse model of fetal alcohol syndrome. Journal of Pharmacology & Experimental Therapeutics, 2001. **297**(2): p. 774-9.
6. Charness, M.E., R.P. Simon, and D.A. Greenberg, Ethanol and the nervous system. N Engl J Med, 1989. **321**: p. 442-54.
7. Diamond, I. and A.S. Gordon, Cellular and molecular neuroscience of alcoholism. Physiol Rev, 1997. **77**(1): p. 1-20.
8. Harris, R.A., Ethanol actions on multiple ion channels: which are important? Alc Clin Exp Res, 1999. **23**: p. 1563-1570.
9. Peoples, R.W., C. Li, and F.F. Weight, Lipid vs protein theories of alcohol action in the nervous system. Ann Rev Pharmacol Toxicol, 1996. **36**: p. 185-201.
10. Franks, N.P. and W.R. Lieb, Do general anaesthetics act by competitive binding to specific receptors? Nature, 1984. **310**(5978): p. 599-601.
11. Slater, S.J., K.J. Cox, J.V. Lombardi, C. Ho, M.B. Kelly, E. Rubin, and C.D. Stubbs, Inhibition of protein kinase C by alcohols and anaesthetics. Nature, 1993. **364**(6432): p. 82-4.
12. Charness, M.E., Direct effects of ethanol on signaling proteins. Alcohol: Clin Exp Res, 1996. **20**: p. 157A-161A.
13. Wick, M.J., S.J. Mihic, S. Ueno, M.P. Mascia, J.R. Trudell, S.J. Brozowski, Q. Ye, N.L. Harrison, and R.A. Harris, Mutations of gamma-aminobutyric acid and glycine receptors change alcohol cutoff: Evidence for an alcohol receptor? Proc Natl Acad Sci (USA), 1998. **95**(11): p. 6504-6509.
14. Mascia, M.P., S.J. Mihic, C.F. Valenzuela, P.R. Schofield, and R.A. Harris, A single amino acid determines differences in ethanol actions on strychnine-sensitive glycine receptors. Molecular Pharmacology, 1996. **50**(2): p. 402-6.
15. Ye, Q., V.V. Koltchine, S.J. Mihic, M.P. Mascia, M.J. Wick, S.E. Finn, N.L. Harrison, and R.A. Harris, Enhancement of glycine receptor function by ethanol is inversely correlated with molecular volume at position alpha267. Journal of Biological Chemistry, 1998. **273**(6): p. 3314-9.
16. Mihic, S.J., Q. Ye, M.J. Wick, V.V. Koltchine, M.D. Krasowski, S.E. Finn, M.P. Mascia, C.F. Valenzuela, K.K. Hanson, E.P. Greenblatt, R.A. Harris, and N.L. Harrison, Sites of alcohol and volatile anaesthetic action on GABA(A) and glycine receptors [see comments]. Nature, 1997. **389**(6649): p. 385-9.
17. Dwyer, D.S. and R.J. Bradley, Chemical properties of alcohols and their protein binding sites. Cell Mol Life Sci, 2000. **57**: p. 265-275.
18. Abel, E.L. and R.J. Sokol, Incidence of fetal alcohol syndrome and economic impact of FAS-related anomalies. Drug Alc Depend, 1987. **19**: p. 51-70.
19. Streissguth, A.P., S. Landesman-Dwyer, J.C. Martin, and D.W. Smith, Teratogenic effects of alcohol in humans and laboratory animals. Science, 1980. **209**: p. 353-361.
20. Sowell, E.R., T.L. Jernigan, S.N. Mattson, E.P. Riley, D.F. Sobel, and K.L. Jones, Abnormal development of the cerebellar vermis in children prenatally exposed to alcohol: size reduction in lobules I-V. Alcohol Clin Exp Res, 1996. **20**: p. 31-34.
21. Clarren, S.K., E.J. Alvord, S.M. Sumi, A.P. Streissguth, and D.W. Smith, Brain malformations related to prenatal exposure to ethanol. J Pediatr, 1978. **92**(1): p. 64-7.
22. Jones, K.L. and D.W. Smith, Recognition of the fetal alcohol syndrome in early infancy. Lancet, 1973. **2**(836): p. 999-1001.
23. Riley, E.P., S.N. Mattson, E.R. Sowall, T.L. Jernigan, D.F. Sobel, and K.L. Jones, Abnormalities of the corpus callosum in children prenatally exposed to alcohol. Alcohol Clin Exp Res, 1995. **19**: p. 1198-1202.
24. Swayze, V.W., 2nd, V.P. Johnson, J.W. Hanson, J. Piven, Y. Sato, J.N. Giedd, D. Mosnik, and N.C. Andreasen, Magnetic resonance imaging of brain anomalies in fetal alcohol syndrome. Pediatrics, 1997. **99**(2): p. 232-40.
25. Stratton, K., C. Howe, and F. Battaglia, Fetal Alcohol Syndrome: Diagnosis, Epidemiology, Prevention, and Treatment. 1996, Washington, D.C.: National Academy Press.
26. Bhave, S.V. and P.L. Hoffman, Ethanol promotes apoptosis in cerebellar granule cells by inhibiting the trophic effect of NMDA. Journal of Neurochemistry, 1997. **68**(2): p. 578-86.
27. Ikonomidou, C., P. Bittigau, M.J. Ishimaru, D.F. Wozniak, C. Koch, K. Genz, M.T. Price, V. Stefovska, F. Horster, T. Tenkova, K. Dikranian, and J.W. Olney, Ethanol-induced apoptotic neurodegeneration and fetal alcohol syndrome. Science, 2000. **287**(5455): p. 1056-60.
28. Dow, K.E. and R.J. Riopelle, Ethanol neurotoxicity: effects on neurite formation and neurotrophic factor production in vitro. Science, 1985. **228**(4699): p. 591-3.

29. Walker, D.W., N. Lee, M.B. Heaton, M.A. King, and B.E. Hunter, Chronic ethanol consumption reduces the neurotrophic activity in rat hippocampus. Neuroscience Letters, 1992. **147**(1): p. 77-80.
30. Roivainen, R., B. Hundle, and R.O. Messing, Ethanol enhances growth factor activation of mitogen-activated protein kinases by a protein kinase C-dependent mechanism. Proc Natl Acad Sci (USA), 1995. **92**: p. 1891-5.
31. Hundle, B., T. McMahon, J. Dadgar, C.H. Chen, D. Mochly-Rosen, and R.O. Messing, An inhibitory fragment derived from protein kinase Cepsilon prevents enhancement of nerve growth factor responses by ethanol and phorbol esters. Journal of Biological Chemistry, 1997. **272**(23): p. 15028-35.
32. Heaton, M.B., D.J. Swanson, M. Paiva, and D.W. Walker, Ethanol exposure affects trophic factor activity and responsiveness in chick embryo. Alcohol, 1992. **9**(2): p. 161-6.
33. Heaton, M.B., M. Paiva, D.J. Swanson, and D.W. Walker, Modulation of ethanol neurotoxicity by nerve growth factor. Brain Research, 1993. **620**(1): p. 78-85.
34. Aloe, L., L. Bracci-Laudiero, and P. Tirassa, The effect of chronic ethanol intake on brain NGF level and on NGF-target tissues of adult mice. Drug & Alcohol Dependence, 1993. **31**(2): p. 159-67.
35. Resnicoff, M., C. Sell, D. Ambrose, R. Baserga, and R. Rubin, Ethanol inhibits the autophosphorylation of the insulin-like growth factor 1 (IGF-1) receptor and IGF-1-mediated proliferation of 3T3 cells. Journal of Biological Chemistry, 1993. **268**(29): p. 21777-82.
36. Bhave, S.V., L. Ghoda, and P.L. Hoffman, Brain-derived neurotrophic factor mediates the anti-apoptotic effect of NMDA in cerebellar granule neurons: signal transduction cascades and site of ethanol action. Journal of Neuroscience, 1999. **19**(9): p. 3277-86.
37. West, J.R., C.R. Goodlett, D.J. Bonthius, K.M. Hamre, and B.L. Marcussen, Cell population depletion associated with fetal alcohol brain damage: mechanisms of BAC-dependent cell loss. Alcoholism: Clinical & Experimental Research, 1990. **14**(6): p. 813-8.
38. Kotch, L.E. and K.K. Sulik, Experimental fetal alcohol syndrome: proposed pathogenic basis for a variety of associated facial and brain anomalies. Am J Med Genet, 1992. **44**(2): p. 168-76.
39. Kotch, L.E. and K.K. Sulik, Patterns of ethanol-induced cell death in the developing nervous system of mice; neural fold states through the time of anterior neural tube closure. Int J Dev Neurosci, 1992. **10**(4): p. 273-9.
40. Kotch, L.E., S.Y. Chen, and K.K. Sulik, Ethanol-induced teratogenesis: free radical damage as a possible mechanism. Teratology, 1995. **52**(3): p. 128-36.
41. Cartwright, M.M. and S.M. Smith, Stage-dependent effects of ethanol on cranial neural crest cell development: partial basis for the phenotypic variations observed in fetal alcohol syndrome. Alcoholism: Clinical & Experimental Research, 1995. **19**(6): p. 1454-62.
42. Cartwright, M.M., L.L. Tessmer, and S.M. Smith, Ethanol-induced neural crest apoptosis is coincident with their endogenous death, but is mechanistically distinct. Alcoholism: Clinical & Experimental Research, 1998. **22**(1): p. 142-9.
43. Cui, S.J., M. Tewari, T. Schneider, and R. Rubin, Ethanol promotes cell death by inhibition of the insulin-like growth factor I receptor. Alcoholism: Clinical & Experimental Research, 1997. **21**(6): p. 1121-7.
44. Liesi, P., Ethanol-exposed central neurons fail to migrate and undergo apoptosis. Journal of Neuroscience Research, 1997. **48**(5): p. 439-48.
45. Zhang, F.X., R. Rubin, and T.A. Rooney, Ethanol induces apoptosis in cerebellar granule neurons by inhibiting insulin-like growth factor 1 signaling. Journal of Neurochemistry, 1998. **71**(1): p. 196-204.
46. Pantazis, N.J., D.P. Dohrman, J. Luo, C.R. Goodlett, and J.R. West, Alcohol reduces the number of pheochromocytoma (PC12) cells in culture. Alcohol, 1992. **9**(3): p. 171-80.
47. Pierce, D.R. and J.R. West, Blood alcohol concentration: a critical factor for producing fetal alcohol effects. Alcohol, 1986. **3**(4): p. 269-72.
48. Pierce, D.R. and J.R. West, Alcohol-induced microencephaly during the third trimester equivalent: relationship to dose and blood alcohol concentration. Alcohol, 1986. **3**(3): p. 185-91.
49. Bonthius, D.J., C.R. Goodlett, and J.R. West, Blood alcohol concentration and severity of microencephaly in neonatal rats depend on the pattern of alcohol administration. Alcohol, 1988. **5**(3): p. 209-14.
50. Maier, S.E., W.J. Chen, J.A. Miller, and J.R. West, Fetal alcohol exposure and temporal vulnerability regional differences in alcohol-induced microencephaly as a function of the timing of binge-like alcohol exposure during rat brain development. Alcoholism: Clinical & Experimental Research, 1997. **21**(8): p. 1418-28.
51. Mitchell, J.J., M. Paiva, and M.B. Heaton, The antioxidants vitamin E and beta-carotene protect against ethanol-induced neurotoxicity in embryonic rat hippocampal cultures. Alcohol, 1999. **17**(2): p. 163-8.

52. Luo, J., J.R. West, R.T. Cook, and N.J. Pantazis, Ethanol induces cell death and cell cycle delay in cultures of pheochromocytoma PC12 cells. Alcoholism: Clinical & Experimental Research, 1999. **23**(4): p. 644-56.
53. Charness, M.E., R.M. Safran, and G. Perides, Ethanol inhibits neural cell-cell adhesion. J Biol Chem, 1994. **269**: p. 9304-9309.
54. Ramanathan, R., M.F. Wilkemeyer, B. Mittal, G. Perides, and M.E. Charness, Ethanol inhibits cell-cell adhesion mediated by human L1. J Cell Biol, 1996. **133**: p. 381-390.
55. Frisch, S.M., K. Vuori, E. Ruoslahti, and P.Y. Chan-Hui, Control of adhesion-dependent cell survival by focal adhesion kinase. Journal of Cell Biology, 1996. **134**(3): p. 793-9.
56. Frisch, S.M. and E. Ruoslahti, Integrins and anoikis. Current Opinion in Cell Biology, 1997. **9**(5): p. 701-6.
57. Li, A.E., H. Ito, Rovira, II, K.S. Kim, K. Takeda, Z.Y. Yu, V.J. Ferrans, and T. Finkel, A role for reactive oxygen species in endothelial cell anoikis. Circulation Research, 1999. **85**(4): p. 304-10.
58. Itoh, K., B. Stevens, M. Schachner, and R.D. Fields, Regulated expression of the neural cell adhesion molecule L1 by specific patterns of neural impulses. Science, 1995. **270**(5240): p. 1369-1372.
59. Wood, P.M., M. Schachner, and R.P. Bunge, Inhibition of Schwann cell myelination in vitro by antibody to the L1 adhesion molecule. Journal of Neuroscience, 1990. **10**(11): p. 3635-45.
60. Kenwrick, S. and P. Doherty, Neural cell adhesion molecule L1: relating disease to function. Bioessays, 1998. **20**(8): p. 668-75.
61. Lüthi, A., J.-P. Laurent, A. Figurov, D. Muller, and M. Schachner, Hippocampal long-term potentiation and neural cell adhesion molecules L1 and NCAM. Nature, 1994. **372**: p. 777-779.
62. Williams, E.J., J. Furness, F.S. Walsh, and P. Doherty, Activation of the FGF receptor underlies neurite outgrowth stimulated by L1, N-CAM, and N-cadherin. Neuron, 1994. **13**(3): p. 583-94.
63. Ignelzi, M., Jr., D.R. Miller, P. Soriano, and P.F. Maness, Impaired neurite outgrowth of src-minus cerebellar neurons on the cell adhesion molecule L1. Neuron, 1994. **12**(4): p. 873-84.
64. Lemmon, V., K.L. Farr, and C. Lagenaur, L1-mediated axon outgrowth occurs via a homophilic binding mechanism. Neuron, 1989. **2**(6): p. 1597-603.
65. Kamiguchi, H. and V. Lemmon, Neural cell adhesion molecule L1: signaling pathways and growth cone motility. J Neurosci Res, 1997. **49**(1): p. 1-8.
66. Hortsch, M., The L1 family of neural cell adhesion molecules: old proteins performing new tricks. Neuron, 1996. **17**(4): p. 587-93.
67. Zhao, X. and C.-H. Siu, Colocalization of the homophilic binding site and the neuritogenic activity of the cell adhesion molecule L1 to its second Ig-like domain. J Biol Chem, 1995. **270**: p. 29413-29421.
68. Holm, J., F. Appel, and M. Schachner, Several extracellular domains of the neural cell adhesion molecule L1 are involved In hemophilic interactions. J Neurosci Res, 1995. **42**(1): p. 9-20.
69. Appel, F., J. Holm, J.F. Conscience, and M. Schachner, Several extracellular domains of the neural cell adhesion molecule L1 are involved in neurite outgrowth and cell body adhesion. J Neurosci, 1993. **13**(11): p. 4764-75.
70. Hortsch, M., Y.M. Wang, Y. Marikar, and A.J. Bieber, The cytoplasmic domain of the Drosophila cell adhesion molecule neuroglian is not essential for its homophilic adhesive properties in S2 cells. J Biol Chem, 1995. **270**(32): p. 18809-17.
71. Zhao, X., P.M. Yip, and C.H. Siu, Identification of a homophilic binding site in immunoglobulin-like domain 2 of the cell adhesion molecule L1. Journal of Neurochemistry, 1998. **71**(3): p. 960-71.
72. Wong, E.V., G. Cheng, H.R. Payne, and V. Lemmon, The cytoplasmic domain of the cell adhesion molecule L1 is not required for homophilic adhesion. Neurosci Lett, 1995. **200**: p. 155-158.
73. De Angelis, E., J. MacFarlane, J.S. Du, G. Yeo, R. Hicks, F.G. Rathjen, S. Kenwrick, and T. Brummendorf, Pathological missense mutations of neural cell adhesion molecule L1 affect homophilic and heterophilic binding activities. EMBO Journal, 1999. **18**(17): p. 4744-53.
74. Haspel, J., D.R. Friedlander, N. Ivgy-May, S. Chickramane, C. Roonprapunt, S. Chen, M. Schachner, and M. Grumet, Critical and optimal Ig domains for promotion of neurite outgrowth by L1/Ng-CAM. Journal of Neurobiology, 2000. **42**(3): p. 287-302.
75. Kadmon, G., A. Kowitz, P. Altevogt, and M. Schachner, The neural cell adhesion molecule N-CAM enhances L1-dependent cell-cell interactions. J Cell Biol, 1990. **110**(1): p. 193-208.
76. Reid, R.A. and J.J. Hemperly, Variants of human L1 cell adhesion molecule arise through alternate splicing of RNA. J Mol Neurosci, 1992. **3**(3): p. 127-35.
77. Kamiguchi, H. and V. Lemmon, A neuronal form of the cell adhesion molecule L1 contains a tyrosine-based signal required for sorting to the

axonal growth cone. Journal of Neuroscience, 1998. **18**(10): p. 3749-56.
78. Takeda, Y., H. Asou, Y. Murakami, M. Miura, M. Kobayashi, and K. Uyemura, A nonneuronal isoform of cell adhesion molecule L1: tissue-specific expression and functional analysis. J Neurochem, 1996. **66**(6): p. 2338-49.
79. Kamiguchi, H., K.E. Long, M. Pendergast, A.W. Schaefer, I. Rapoport, T. Kirchhausen, and V. Lemmon, The neural cell adhesion molecule L1 interacts with the AP-2 adaptor and is endocytosed via the clathrin-mediated pathway. Journal of Neuroscience, 1998. **18**(14): p. 5311-21.
80. De Angelis, E., T. Brummendorf, L. Cheng, V. Lemmon, and S. Kenwrick, Alternative use of a mini exon of the L1 gene affects L1 binding to neural ligands. Journal of Biological Chemistry, 2001. **276**(35): p. 32738-42.
81. Hortsch, M., K.S. O'Shea, G. Zhao, F. Kim, Y. Vallejo, and R.R. Dubreuil, A conserved role for L1 as a transmembrane link between neuronal adhesion and membrane cytoskeleton assembly. Cell Adhesion & Communication, 1998. **5**(1): p. 61-73.
82. Garver, T.D., Q. Ren, S. Tuvia, and V. Bennett, Tyrosine phosphorylation at a site highly conserved in the L1 family of cell adhesion molecules abolishes ankyrin binding and increases lateral mobility of neurofascin. J Cell Biol, 1997. **137**(3): p. 703-14.
83. Tuvia, S., T.D. Garver, and V. Bennett, The phosphorylation state of the FIGQY tyrosine of neurofascin determines ankyrin-binding activity and patterns of cell segregation. Proceedings of the National Academy of Sciences of the United States of America, 1997. **94**(24): p. 12957-62.
84. Rader, C., B. Kunz, R. Lierheimer, R.J. Giger, P. Berger, P. Tittmann, H. Gross, and P. Sonderegger, Implications for the domain arrangement of axonin-1 derived from the mapping of its NgCAM binding site. EMBO Journal, 1996. **15**(9): p. 2056-68.
85. Kunz, S., M. Spirig, C. Ginsburg, A. Buchstaller, P. Berger, R. Lanz, C. Rader, L. Vogt, B. Kunz, and P. Sonderegger, Neurite fasciculation mediated by complexes of axonin-1 and Ng cell adhesion molecule. Journal of Cell Biology, 1998. **143**(6): p. 1673-90.
86. Friedlander, D.R., P. Milev, L. Karthikeyan, R.K. Margolis, R.U. Margolis, and M. Grumet, The neuronal chondroitin sulfate proteoglycan neurocan binds to the neural cell adhesion molecules Ng-CAM/L1/NILE and N-CAM, and inhibits neuronal adhesion and neurite outgrowth. J Cell Biol, 1994. **125**(3): p. 669-80.
87. Oleszewski, M., S. Beer, S. Katich, C. Geiger, Y. Zeller, U. Rauch, and P. Altevogt, Integrin and neurocan binding to L1 involves distinct Ig domains. Journal of Biological Chemistry, 1999. **274**(35): p. 24602-10.
88. Fransen, E., V. Lemmon, G. Vancamp, L. Vits, P. Coucke, and P.J. Willems, CRASH syndrome - Clinical spectrum of corpus callosum hypoplasia, retardation, adducted thumbs, spastic paraparesis and hydrocephalus due to mutations in one single gene, L1 [Review]. Eur J Hum Genet, 1995. **3**(5): p. 273-284.
89. Fransen, E., R. Dhooge, G. Vancamp, M. Verhoye, J. Sijbers, E. Reyniers, P. Soriano, H. Kamiguchi, R. Willemsen, S.K.E. Koekkoek, C.I. Dezeeuw, P.P. Dedeyn, A. Vanderlinden, V. Lemmon, R.F. Kooy, and P.J. Willems, L1 knockout mice show dilated ventricles, vermis hypoplasia and impaired exploration patterns. Human Mol Genet, 1998. **7**(6): p. 999-1009.
90. Demyanenko, G.P., A.Y. Tsai, and P.F. Maness, Abnormalities in neuronal process extension, hippocampal development, and the ventriclar system of L1 knockout mice. J Neurosci, 1999. **19**: p. 4907-4920.
91. Luo, J. and M.W. Miller, Transforming growth factor beta1-regulated cell proliferation and expression of neural cell adhesion molecule in B104 neuroblastoma cells: differential effects of ethanol. Journal of Neurochemistry, 1999. **72**(6): p. 2286-93.
92. Wilkemeyer, M.F., M. Pajerski, and M.E. Charness, Alcohol inhibition of cell adhesion in BMP-treated NG108-15 cells. Alcohol Clin Exp Res, 1999. **23**: p. 1711-1720.
93. Wilkemeyer, M.F. and M.E. Charness, Characterization of alcohol-sensitive and insensitive fibroblast cell lines expressing human L1. J Neurochem, 1998. **71**: p. 2382-2391.
94. Bearer, C.F., A.R. Swick, M.A. O'Riordan, and G. Cheng, Ethanol inhibits L1-mediated neurite outgrowth in postnatal rat cerebellar granule cells. J Biol Chem, 1999. **274**: p. 13264-13270.
95. Vallejo, Y., M. Hortsch, and R.R. Dubreuil, Ethanol does not inhibit the adhesive activity of Drosophila neuroglian or human L1 in Drosophila S2 tissue culture cells. J Biol Chem, 1997. **272**(18): p. 12244-7.
96. Zhao, X. and C.H. Siu, Differential effects of two hydrocephalus/MASA syndrome-related mutations on the homophilic binding and neuritogenic activities of the cell adhesion molecule L1. J Biol Chem, 1996. **271**(12): p. 6563-6.
97. Brenneman, D.E. and G.A. Foster, Structural specificity of peptides influencing neuronal survival during development. Peptides, 1987. **8**(4): p. 687-94.
98. Brenneman, D.E., C.Y. Spong, and I. Gozes, Protective peptides derived from novel glial proteins. Biochemical Society Transactions, 2000. **28**(4): p. 452-5.

99. Brenneman, D.E., J. Hauser, E. Neale, S. Rubinraut, M. Fridkin, A. Davidson, and I. Gozes, Activity-dependent neurotrophic factor: structure-activity relationships of femtomolar-acting peptides. Journal of Pharmacology & Experimental Therapeutics, 1998. **285**(2): p. 619-27.
100. Steingart, R.A., B. Solomon, D.E. Brenneman, M. Fridkin, and I. Gozes, VIP and peptides related to activity-dependent neurotrophic factor protect PC12 cells against oxidative stress. Journal of Molecular Neuroscience, 2000. **15**(3): p. 137-45.
101. Offen, D., Y. Sherki, E. Melamed, M. Fridkin, D.E. Brenneman, and I. Gozes, Vasoactive intestinal peptide (VIP) prevents neurotoxicity in neuronal cultures: relevance to neuroprotection in Parkinson's disease. Brain Research, 2000. **854**(1-2): p. 257-62.
102. Wilkemeyer, M.F., C. Menkari, C.Y. Spong, and M.E. Charness, Peptide antagonists of ethanol inhibition of L1-mediated cell-cell adhesion. J Pharmacol Exp Ther, 2002. **303**: p. 110-116.
103. Miller, K., G. Addona, and M. Kloczewiak, Approaches to proving there are general anesthetic sites on ligand gated ion channels. General Pharmacology, 1998.
104. Forman, S.A., K.W. Miller, and G. Yellen, A discrete site for general anesthetics on a postsynaptic receeptor. Molecular Pharmacology, 1995. **48**: p. 1-8.
105. Mihic, S.J., Y. Qing, M.J. Wick, V.V. Koltchine, M.D. Krasowski, S.E. Finn, M.P. Mascia, C.F. Valenzuela, K.K. Hanson, E.P. Greenblatt, R.A. Harris, and N.L. Harrison, Sites of alcohol and volatile anaesthetic action on GABAa and Glycine receptors. NAture, 1997. **389**: p. 385-389.
106. Wood, S.C., P.H. Tonner, A.A. de, B. Bugge, and K.W. Miller, Channel inhibition by alkanols occurs at a binding site on the nicotinic acetylcholine receptor. Molecular Pharmacology, 1995. **47**(1): p. 121-30.
107. Bertrand, D. and J.P. Changeux, Nicotinic receptor: a prototype of allosteric ligand-gated ion channels and its possible implications in epilepsy. [Review] [164 refs]. Advances in Neurology, 1999. **79**(171): p. 171-88.
108. Changeux, J.P., J.L. Galzi, A. Devillers-Thiery, and D. Bertrand, The functional architecture of the acetylcholine nicotinic receptor explored by affinity labelling and site-directed mutagenesis. Quarterly Reviews Biophysics, 1992. **25**: p. 395-432.
109. Husain, S.S., S.A. Forman, M.A. Kloczewiak, G.H. Addona, R.W. Olsen, M.B. Pratt, J.B. Cohen, and K.W. Miller, Synthesis and properties of 3-(2-hydroxyethyl)-3-n-pentyldiazirine, a photoactivable general anesthetic. Journal of Medicinal Chemistry, 1999. **42**(17): p. 3300-7.
110. Bayley, H., Photogenerated Reagents in Biochemistry and Molecular Biology, ed. T.S. Work and R.H. Burdon. 1983, New York: Elsevier.
111. Brunner, B., New photolabeling and crosslinking methods. Annu. Rev. Biochem., 1993. **62**: p. 483-514.
112. Husain, S.S., S.A. Forman, M.A. Kloczewiak, G.H. Addona, R.W. Olsen, M.B. Pratt, J.B. Cohen, and K.W. Miller, Synthesis and properties of 3-(2-hydroxyethyl)-3-n-pentyldiazirine, a photoactivable general anesthetic. J Med Chem, 1999. **42**(17): p. 3300-7.
113. Pratt, M.B., S.S. Husain, K.W. Miller, and J.B. Cohen, Identification of sites of incorporation in the nicotinic acetylcholine receptor of a photoactivatible general anesthetic. J Biol Chem, 2000. **275**(38): p. 29441-51.
114. Sampath, T.K., J.E. Coughlin, R.M. Whetstone, D. Banach, C. Corbett, R.J. Ridge, E. Özkaynak, H. Oppermann, and D.C. Rueger, Bovine osteogenic protein is composed of dimers of OP-1and BMP-2A, two members of the transforming growth factor-ß superfamily. J Biol Chem, 1990. **265**: p. 13198-13205.
115. Sampath, T.K., J.C. Maliakal, P.V. Hauschka, W.K. Jones, H. Sasak, R.F. Tucker, K.H. White, J.E. Coughlin, M.M. Tucker, R.H. Pang, C. Corbett, E. Özkaynak, H. Opperman, and D.C. Rueger, Recombinant human osteogenic protein-1 (hOP-1) induces new bone formation in vivo with a specific activity comparable with natural bovine osteogenic protein and stimulates osteoblast proliferation and differentiation in vitro. J Biol Chem, 1992. **267**(28): p. 20352-20362.
116. Lyons, K.M., R.W. Pelton, and B.L. Hogan, Organogenesis and pattern formation in the mouse: RNA distribution patterns suggest a role for bone morphogenetic protein-2A (BMP-2A). Development, 1990. **109**(4): p. 833-44.
117. Jones, C.M., K.M. Lyons, and B.L. Hogan, Involvement of Bone Morphogenetic Protein-4 (BMP-4) and Vgr-1 in morphogenesis and neurogenesis in the mouse. Development, 1991. **111**(2): p. 531-542.
118. Perides, G., R.M. Safran, D.C. Rueger, and M.E. Charness, Induction of the neural cell adhesion molecule and neuronal aggregation by osteogenic protein 1. Proc Natl Acad Sci (USA), 1992. **89**: p. 10326-10330.
119. Perides, G., G. Hu, D.C. Rueger, and M.E. Charness, Osteogenic protein-1 regulates L1 and neural cell adhesion molecule gene expression in neural cells. J Biol Chem, 1993. **268**: p. 25197-25205.

120. Perides, G., R.M. Safran, L.A. Downing, and M.E. Charness, Regulation of N-CAM and L1 by the TGF-ß superfamily: selective effects of the bone morphogenetic proteins. J Biol Chem, 1994. **269**: p. 765-770.
121. Asou, H., M. Miura, M. Kobayashi, K. Uyemura, and K. Itoh, Cell adhesion molecule L1 guides cell migration in primary reaggregation cultures of mouse cerebellar cells. Neurosci Lett, 1992. **144**: p. 221-224.
122. Pollerberg, E.G., R. Sadoul, C. Goridis, and M. Schachner, Selective expression of the 180-kD component of the neural cell adhesion molecule N-CAM during development. Journal of Cell Biology, 1985. **101**(5 Pt 1): p. 1921-9.
123. McCreery, M.J. and W.A. Hunt, Physico-chemical correlates of alcohol intoxication. Neuropharmacol, 1978. **17**(7): p. 451-61.
124. Wilkemeyer, M.F., C.E. Menkari, and M.E. Charness, Novel antagonists of alcohol inhibition of L1-mediated cell adhesion: multiple mechanisms of action. Mol Pharmacol, 2002. **62**(11): p. 1053-1060.
125. Wilkemeyer, M.F., S.Y. Chen, C.E. Menkari, D.E. Brenneman, K.K. Sulik, and M.E. Charness, Differential Effects of Ethanol Antagonism and Neuroprotection in NAP Prevention of Ethanol-induced Developmental Toxicity. Proc.Natl. Acad. Sci. U.S.A., 2003, submitted.
126. Hunt, D.F., J.R. Yates, 3rd, J. Shabanowitz, S. Winston, and C.R. Hauer, Protein sequencing by tandem mass spectrometry. Proc Natl Acad Sci U S A, 1986. **83**(17): p. 6233-7.
127. Addona, G., S. Husain, and K. Miller, Identification of the Contact Residue Between Adenylate Kinase and the General Anesthetic 3,3-Azioctan-1-ol by Mass Spectrometry. *Biophysical Journal*, 1999. **76**: p. A103.
128. Addona, G.H., S.S. Husain, and K.W. Miller, The Topography Of An Anesthetic Binding Site In Adenylate Kinase Using Photoreactive Anesthetics And Mass Spectrometry. Biophysics J., 2001. **80**: p. 314a.
129. Addona, G., W. Sandberg, and K. Miller, Location of a General Anesthetic Binding Site In Protein Kinase C Cys-2 Region Identified by Photoaffinity Labeling and Mass Spectrometry. Anesthesiology 2000; (Electronic publication)., 2000.
130. Sachsenheimer, W., E.F. Pai, G.E. Schulz, and R.H. Schirmer, Halothane binds in the adenine-specific niche of crystalline adenylate kinase. FEBS Lett, 1977. **79**(2): p. 310-2.
131. Yan, H. and M.D. Tsai, Nucleoside monophosphate kinases: structure, mechanism, and substrate specificity. Advances in Enzymology & Related Areas of Molecular Biology, 1999. **73**: p. 103-34.
132. Dreusicke, D., P.A. Karplus, and G.E. Schulz, Refined structure of porcine cytosolic adenylate kinase at 2.1 A resolution. J Mol Biol, 1988. **199**(2): p. 359-71.
133. Muller, C.W. and G.E. Schulz, Structure of the complex between adenylate kinase from Escherichia coli and the inhibitor Ap5A refined at 1.9 A resolution. A model for a catalytic transition state. Journal of Molecular Biology, 1992. **224**(1): p. 159-77.
134. Wolff, J.M., R. Frank, K. Mujoo, R.C. Spiro, R.A. Reisfeld, and F.G. Rathjen, A human brain glycoprotein related to the mouse cell adhesion molecule L1. Journal of Biological Chemistry, 1988. **263**(24): p. 11943-7.
135. Sadoul, K., R. Sadoul, A. Faissner, and M. Schachner, Biochemical characterization of different molecular forms of the neural cell adhesion molecule L1. Journal of Neurochemistry, 1988. **50**(2): p. 510-21.
136. Hortsch, M., Structural and functional evolution of the L1 family: are four adhesion molecules better than one? Molecular & Cellular Neurosciences, 2000. **15**(1): p. 1-10.
137. Bateman, A., M. Jouet, J. MacFarlane, J.S. Du, S. Kenwrick, and C. Chothia, Outline structure of the human L1 cell adhesion molecule and the sites where mutations cause neurological disorders. Embo J, 1996. **15**(22): p. 6050-9.
138. Grumet, M., Cell adhesion molecules and their subgroups in the nervous system. Current Opinion in Neurobiology., 1991. **1**(3): p. 370-6.
139. Haspel, J., C. Blanco, J. Jacob, and M. Grumet, System for cleavable Fc fusion proteins using tobacco etch virus (TEV) protease. Biotechniques, 2001. **30**(1): p. 60-1, 64-6.
140. Sakurai, T., C. Roonprapunt, and M. Grumet, Purification of Ig-fusion proteins from medium containing Ig. Biotechniques., 1998. **25**(3): p. 382-5.
141. Addona, G.H., S.S. Husain, T. Stehle, and K.W. Miller, Geometric isomers of a photoactivatible general anesthetic delineate a binding site on adenylate kinase. J. Biol. Chem., 2002: p. in press.
142. Pratt, M.B., S.S. Husain, K.W. Miller, and J.B. Cohen, Identification of sites of incorporation in the nicotinic acetylcholine receptor of a photoactivatible general anesthetic. J Biol Chem, 2000. **275**(38): p. 29441-29451.
143. Miller, K., *Multiple actions of ethanol on acetylcholine receptors*, in *Alcohol, Cell Membranes, and Signal Transduction in Brain-3/16/94*, D.I. Alling C, Leslie S, Sun G, and Wood WG, Editors. 1993, Plenum Press: New York. p. 83-96.
144. Chiara, D.C., M.A. Kloczewiak, G.H. Addona, J.A. Yu, J.B. Cohen, and K.W. Miller, Site of